CONTENTS R through S

Formation Interval of the Lunar Mantle from High-Precision Nd-Isotope Measurements of Six Lunar Basalts
K. Rankenburg, A. D. Brandon, and C. R. Neal 5036

GENTNER — A Miniaturised LIBS/Raman Instrument for the Comprehensive In Situ Analysis of the Martian Surface
I. Rauschenbach, V. Lazic, E. K. Jessberger, and GENTNER Team 5224

Updates of Proton Cross Sections for Producing Cosmogenic Radionuclides
R. C. Reedy and K. J. Kim 5346

Radiogenic and Stable Thallium Isotope Variations in Iron Meteorites
M. Rehkämper, S. G. Nielsen, H. M. Williams, M. Schönbächler, and A. N. Halliday 5062

Milton Pallasite and the South Byron Iron Trio: A Grouplet Formed by Oxidation and Fractional Crystallization
V. S. Reynolds, T. J. McCoy, and W. F. McDonough 5233

Mineralogy and Petrology of the Mare Basalt-rich Breccia MET 01210
K. Righter and B. Bussey 5364

The Great Diversity of Planetary Materials Returned from the Queen Alexandra Range, Antarctica
K. Righter, R. P. Harvey, J. W. Schutt, C. Satterwhite, K. M. McBride, T. J. McCoy, and L. Welzenbach 5363

Revisiting the Decompressed Density of Mercury
M. A. Riner, C. R. Bina, and M. S. Robinson 5377

Variations in Lunar Opaque Phase and Grain Size: Implications for Remote Sensing of TiO_2
M. A. Riner, M. S. Robinson, P. G. Lucey, and D. S. Ebel 5339

The Molecular Structure and Isotopic Compositions of the Insoluble Organic Matter in Chondrites
F. Robert and S. Derenne 5259

A Catalogue of Large Meteorite Specimens from Campo Del Cielo Meteorite Shower, Cahco Province, Argentina
M. C. L. Rocca 5001

Two New Potential Meteorite Impact Sites in Chubut Province, Argentina
M. C. L. Rocca 5002

Magnetic Classification, Weathering and Terrestrial Ages of Antarctic Ordinary Chondrites
P. Rochette, L. Folco, J. Gattacceca, C. Berteloot, and C. Suavet 5191

Magnetic Classification of C, E, K, R and Ungrouped Chondrites
P. Rochette, J. Gattacceca, L. Sagnotti, L. Folco, G. Consolmagno, and M. Denise 5074

SRTM Investigation of the Araguainha Impact Crater, Central Brazil
R. Romano, G. R. Cooper, and W. U. Reimold 5282

The Nature of the Lithium-rich Phase Found in MIL 03346 Mesostasis
D. Rost, E. P. Vicenzi, M. Fries, and A. Steele 5164

Oxidation State and O-Isotopic Compositions of Equilibrated H Chondrites
A. E. Rubin 5271

Shock and Annealing in EL Chondrites
A. E. Rubin 5274

Al-26 in Semarkona (LL3.0) Chondrules: Onset and Duration of Chondrule Formation
N. G. Rudraswami, B. K. Chattopadhyay, B. K. Bandopadhyay, and J. N. Goswami 5091

NWA 2999 and Other Angrites: No Compelling Evidence for a Mercurian Origin
A. Ruzicka and M. Hutson 5080

Trace-Element Compositions of Normal, Dusty, and Clear Olivine in Chainpur Chondrules
A. Ruzicka, C. Floss, and M. Hutson 5266

SEM-CL Study of Quartz from Mt. Oikeyama — Evidences on a Possible Impact Structure in Japan
M. Sakamoto, H. Nishido, A. Gucsik, K. Ninagawa, and T. Okumura 5106

Chicxulub Ejecta Plume Formation and the Link with the Global K-P Boundary
T. Salge, L. Hecht, and D. Stöffler 5228

On Planetesimal Melting and Chronology
I. S. Sanders 5206

Thermal Outgassing of Ordinary Chondritic Material — II. Sensitivity Studies
L. Schaefer and B. Fegley Jr. 5277

Comparison of HSE in Earth and Moon
G. H. Schmidt 5023

The Disruption of the L Chondrite Parent Body and the Great Ordovician Biodiversification Event
B. Schmitz 5052

The Pd-Ag Chronometer and Early Planetary Differentiation
M. Schönbächler, R. W. Carlson, and E. H. Hauri 5330

A Stony Meteorite Discovered by the Mars Exploration Rover Opportunity on Meridiani Planum, Mars
C. Schröder, R. Gellert, B. L. Jolliff, G. Klingelhöfer, T. J. McCoy, R. V. Morris, D. S. Rodionov, P. A. de Souza Jr., A. S. Yen, and J. Zipfel 5285

Large W-182 Excesses in Silicate Inclusions of IAB Iron Meteorites
T. Schulz, C. Muenker, K. Mezger, and H. Palme 5293

New Data on the Cooling History of the H Chondrite Parent Body
W. H. Schwarz, M. Trieloff, E. V. Korochantseva, and A. I. Buikin 5132

Nitrogen and Noble Gases in ALHA 77005, A Small Martian Meteorite From Antarctica
S. P. Schwenzer, S. Herrmann, and U. Ott 5013

Meteoritical and Dynamical Constraints on Formation Mechanisms for Asteroids and Planets
E. R. D. Scott 5353

The Magmatism on Mars Inferred from Chemical Compositions of Martian Meteorites
N. Shirai and M. Ebihara 5251

Airbursts in the Earth's Atmosphere: Application to the 1908 Tunguska Event
V. V. Shuvalov 5057

Statistical Assessment of Major Element Composition of Moldavites from the Cheb Basin
R. Skála 5240

'The Curator's Dilemma' Revisited — Challenges for Meteorite Collections in the 21st Century
C. L. Smith and L. C. Welzenbach 5238

Simultaneous Accretion of Differentiated or Metamorphosed Asteroidal Clasts and Chondrules
A. K. Sokol and A. Bischoff 5042

Percolation of Fe-FeS Melts Through an Olivine Matrix. A Study with a Centrifuging Piston Cylinder
G. Solferino, N. Bagdassarov, and M. W. Schmidt 5179

The Glue That Binds: Consolidation Processes for Planetary Materials
J. G. Spray 5165

Analogous Experiments on Chondrule Formation Using Rapid IR-Laser Heating
T. Springborn, T. Poppe, C. Güttler, J. Blum, and J. Wasson 5123

The Distribution of Inclusions in a Single Large Presolar Silicon Carbide Grain
F. J. Stadermann, T. Stephan, A. S. Lea, and C. Floss 5338

Mineralogy and Petrology of Comet Wild2 Nucleus Samples – Final Results of the Preliminary Examination Team
Stardust Mineralogy/Petrology Subteam, M. Zolensky, P. Bland, J. Bradley, A. Brearley, S. Brennan, J. Bridges, D. Brownlee, A. Butterworth, Z. Dai, D. Ebel, M. Genge, M. Gounelle, G. Graham, J. Grossman, L. Grossman, R. Harvey, H. Ishii, A. Kearsley, L. Keller, A. Krot, F. Langenhorst, A. Lanzirotti, H. Leroux, G. Matrajt, K. Messenger, T. Mikouchi, T. Nakamura, K. Ohsumi, K. Okudaira, M. Perronnet, F. Rietmeijer, S. Simon, T. Stephan, R. Stroud, M. Taheri, K. Tomeoka, A. Toppani, P. Tsou, A. Tsuchiyama, M. Velbel, I. Weber, M. Weisberg, A. Westphal, H. Yano, and T. Zega 5344

Time Dependant Enrichment of Uranium in Oman Desert Chondrites
Ch. Stenger, U. Krähenbühl, and B. A. Hofmann 5139

Terrestrial Analogs for Meteoritic Porosity Measurements
M. M. Strait, G. J. Consolmagno, and D. T. Britt 5171

Supernova Nierite (a-Si_3N_4) from Murchison
R. M. Stroud, L. R. Nittler, and C. M. O'D. Alexander 5360

Numerical Modeling of Tektite Origin in Vertical Impacts
V. V. Svetsov 5065

Ar-Ar Dating of Shock-melted H Chondrites
T. D. Swindle, D. A. Kring, C. Isachsen, E. K. Olson, and J. R. Weirich 5117

FORMATION INTERVAL OF THE LUNAR MANTLE FROM HIGH-PRECISION ND-ISOTOPE MEASUREMENTS OF SIX LUNAR BASALTS.

K. Rankenburg[1], A. D. Brandon[1] and C. R. Neal[2]. [1]NASA Johnson Space Center, Mailcode KR, 2101 Nasa Road One, Houston, TX 77058, kai.rankenburg1@jsc.nasa.gov, [2]Dept. of Civil Eng. & Geological Sciences, University of Notre Dame, Notre Dame, IN 46556, neal.1@nd.edu.

Introduction: If the Moon has superchondritic $^{142}Nd/^{144}Nd$ identical to the Earth, as suggested by available data [1,2], then the giant impact must have occurred into an already differentiated Earth, predominantly sampling the LREE-depleted reservoir. In order to test this hypothesis, Nd-isotope ratios were obtained on a Thermo-Finnigan Triton TIMS for six lunar basalts that span the compositional range of lavas from the Moon: 15555, LAP 02205: low-Ti; 70017, 74275: high-Ti; 15386, SAU 169: KREEP basalts. The lunar samples have crystallization ages of 3.15 to 3.9 Ga and preserve a range of present-day $\varepsilon^{142}Nd$ from -0.30 ± 0.07 (2σ) to +0.07 ± 0.05 when corrected for the effects of neutron irradiation.

The evolution of the lunar mantle is modeled assuming formation from material with average chondritic composition with present day $\varepsilon^{143}Nd = 0$ and $\varepsilon^{142}Nd = -0.2$ [1]. The $\varepsilon^{143}Nd$ and $\varepsilon^{142}Nd$ of the evolving lunar mantle is calculated using a two-stage model [2]. Self-consistent values of $(^{147}Sm/^{144}Nd)_{t1}$ and t_1 are calculated for each sample by simultaneously solving the equations for the evolution of ^{142}Nd and ^{143}Nd. The best fit to the data yields a source formation age of all basalt samples of 215 +23,-21 m.y. (2σ) after solar system formation, and an intercept at the chondritic $^{147}Sm/^{144}Nd$ of = -0.19 ± 0.02 (MSWD= 0.99), consistent with contemporaneous formation of the source regions represented in this study from a LMO with a present day $\varepsilon^{142}Nd = -0.19$.

A model in which the Moon was formed from material that predominantly sampled the Nd-depleted reservoir of an already differentiated Earth and/or impactor, is not consistent with the data. Because both Earth and Moon likely formed in the same region of the solar nebula, the Earth should also have a chondritic bulk composition. In order to mass balance the Nd budget, these constraints require that a complementary reservoir with lower $^{142}Nd/^{144}Nd$ resides in the Earth's mantle.

References:

[1] M. Boyet, R. W. Carlson, *Science* **309**, 576 (2005). [2] L. E. Nyquist et al., *GCA* **59**, 2817 (1995).

GENTNER – A MINIATURISED LIBS/RAMAN INSTRUMENT FOR THE COMPREHENSIVE *IN SITU* ANALYSIS OF THE MARTIAN SURFACE.

I. Rauschenbach[1], V. Lazic[2], E.K. Jessberger[1] and the GENTNER Team. [1]Institut für Planetologie, Westfälische Wilhelms-Universität Münster, Germany. E-mail: irausch@uni-muenster.de. [2]ENEA, Frascati (RM), Italy.

We introduce a novel instrument to determine *in-situ* rapidly and with relatively high sensitivity (down to 10 ppm) the concentrations of many elements in Martian rock, coarse fine and soil samples with a lateral resolution of <1 mm. At the same time the instrument will provide information on possible organic components as well as mineralogical information. Detection of the life-related elements like H, C, N, O, P, S and Fe and investigation of their 3D-distributions as well as their occurrences in the various Martian materials may be indicative of biological activity [1].

The proposed instrument is a combination of Laser Induced Breakdown Spectroscopy (LIBS) and Raman Spectroscopy. It is named GENTNER honouring the german physicist and cosmochemist Wolfgang Gentner (1906 – 1980). GENTNER meets the requirements concerning advanced in situ analytical tools, like short measurement duration, high sensitivity, high repetition rate, high reproducibility, low mass, size and resource needs and high flexibility with respect to type, shape and size of sample material. This innovative instrument, the combination of LIBS with Raman, greatly profits from synergetic effects, sharing the optical spectrometer, the lasers, and onboard data reduction facilities [2]. It also gains from recent developments in miniaturisation and from front-line laser research.

The basic GENTNER concept consists of one or more small, light-weight Sensor Heads mounted on an arm and/or near the tip of a drill, and an Instrument Module (pump lasers, spectrometer, electronics, etc.) installed on a rover. Optical fibres connect Sensor Heads and Instrument Module. An essential feature is the non-prerequisite of sample preparation. GENTNER will perform hundreds of individual chemical, mineralogical and "organic" analyses of all sample types within reach at all geologic sites visited. Distant geologic units are accessible through the analysis of wind- and impact-transported individual coarse fines (approx. 1 mm) samples. These analyses will not be obstructed by dust coverage since the instrument allows depth profiling for up to 2 mm. At the same time GENTNER shall serve to grossly characterize samples prior to GC-MS and isotopic studies in order to preselect interesting samples for these experiments [3].

However, the variability of the environmental conditions on Mars and the differences of the physical-chemical characteristics of the expected samples, require extensive studies of LIBS and Raman spectroscopy under Martian conditions. To obtain reliable quantitative LIBS results and to optimize the LIBS system performance we studied in a first step the influence (a) of sample temperature and (b) of physical status – rock or powder.

References:[1] Bertrand R., Del Bianco A., Jessberger E. K., Mann I., Peuser P., Rost D., Schneider K., Stephan T., Weber, I. 2003. *Flight Model Instrument Concept, LIRAMIS-TN22-03, issue 1.0, ESTEC Contract No.: 16475/02/NL/HB.* [2] Bertrand R., Del Bianco A., Jessberger E. K., Mann I., Peuser P., Rost D., Schneider K., Stephan T., Weber, I. 2003. *LIRAMIS Instrument Definition Document. LIRAMIS-TN4-10c, Issue 1.0.* [3] Bertrand R., Del Bianco A., Jessberger E. K., Mann I., Peuser P., Rost D., Schneider K., Stephan T., Weber, I. 2001. *Technical Data Package. ESTEC Contract no. 14866/00/NL/LVH.*

UPDATES OF PROTON CROSS SECTIONS FOR PRODUCING COSMOGENIC RADIONUCLIDES.

R. C. Reedy[1] and K. J. Kim[2]. [1]Institute of Meteoritics, University of New Mexico, Albuquerque, NM 87131 USA. E-mail: rreedy@unm.edu. [2]NSF-Arizona AMS Laboratory, Physics Building, University of Arizona, Tucson, AZ 85721 USA.

Introduction: Good models are needed to interpret concentrations of cosmogenic nuclides measured in samples of solar-system matter. Theoretical calculations are usually used to get production rates to compare with measurements. Important inputs to these theoretical calculations are cross sections for making the nuclide of interest from its major target elements. Protons make almost all nuclides produced by solar energetic particles and a fraction of the nuclides made by galactic-cosmic-ray (GCR) particles [1]. Most GCR-produced nuclides are made by neutrons, and cross sections for protons reactions are often used for neutrons or as a basis for estimating neutron cross sections.

Proton Reactions Making Cosmogenic Radionuclides: Many cross sections for proton-induced reactions have been measured in the last decade and were included in these evaluations of cross sections for making cosmogenic nuclides. As the first phase of a project to update the cross sections used for our theoretical models, we are doing the major radioactive cosmogenic nuclides ^{10}Be, ^{26}Al, and ^{36}Cl, which are major radionuclides made both by solar protons and GCR particles.

Many cross sections for making these radionuclides for a range of targets and for energies from threshold to ~1 GeV were published in the late 1990s by R. Michel and co-workers [e.g., 2] and by J. Sisterson and colleagues [e.g., 3,4]. We also compiled cross sections from earlier works and searched several archives for additional measurements.

Evaluation: The compiled cross sections for these radionuclides were plotted as a function of energy for each major target element. An evaluated set of cross sections as a function of energy was generated. Often the data from the two major groups were in good agreement. Occasionally, there was some spread in their cross sections for an energy. If there were no other measurements, a smoothed curve that was roughly an average of the different measurements was adopted.

Summary: Revised cross sections as a function of energy have been evaluated for the main proton reactions making ^{10}Be, ^{26}Al, and ^{36}Cl. These cross sections will be used to reinterpret profiles of these radionuclides measured in the top centimeter or so of lunar rocks, such as 64455 [5]. Proton cross sections for other nuclides will be compiled and evaluated. These proton cross sections will also be used as starting points for estimating improved cross sections for neutron-induced cross sections.

References: [1] Reedy R. C. and Arnold J. R. 1972. *Journal of Geophysical Research* 77:537-555. [2] Michel R. et al. 1997. *Nuclear Instruments & Methods B* 129:153-193. [3] Sisterson J. M. et al. 1997. *Nuclear Instruments & Methods B* 123:324-329. [4] Sisterson J. M. et al. 1997. *American Institute of Physics Conference Proceedings* 392:811-814. [5] Nishiizumi K. et al. 1995. 26th Lunar and Planetary Science Conference. pp. 1055-1056.

RADIOGENIC AND STABLE THALLIUM ISOTOPE VARIATIONS IN IRON METEORITES

M. Rehkämper[1], S.G. Nielsen[2], H.M. Williams[2], M. Schönbächler[1], A.N. Halliday[3]. [1]Dept. of Earth Science & Engineering, Imperial College, London SW7 2AZ, UK. [2]Dept. of Earth and Planetary Sciences, Macquarie University, 2109 NSW, Australia. [3]Dept. of Earth Sciences, University of Oxford, Oxford OX1 3PR, UK.

The short-lived radionuclide ^{205}Pb decays to ^{205}Tl with a half-life of 15 Myrs. Evidence for the presence of live ^{205}Pb in the early solar system was provided by a recent Tl isotope study [1], which established a ^{205}Pb-^{205}Tl isochron for seven metal fragments from the IAB irons Toluca and Canyon Diablo. Five troilites from the same meteorites do not conform to the isochron relationships exhibited by the metal samples. In particular, four of the sulfides exhibit Tl isotope compositions that are significantly less radiogenic than the co-existing metals. In studies of extinct radionuclides it has been standard practice to use the least radiogenic isotope ratio measured as the best approximation of the solar system initial. This assumption is questionable for the ^{205}Pb–^{205}Tl decay system, however, because it is difficult to account for the large isotopic contrast between metals and sulfides (up to about 5‰) by radiogenic decay of ^{205}Pb alone.

Mass dependent isotope fractionations provide an alternative explanation for the troilite data and such stable isotope effects have recently been identified in iron meteorites for Fe [2] and Ni [3]. Sulfides from various irons have a mean Fe isotope composition that is isotopically lighter than the metal by 0.5 ± 0.2‰ (1sd) for ^{57}Fe/^{54}Fe, and this offset is most readily explained by equilibrium fractionation. This suggests that the much larger Tl isotope differences between metals and troilites are unlikely reflect equilibrium isotope effects. Rather, they are thought to be due to kinetic fractionations that were generated by diffusion.

This interpretation follows from studies of the extinct ^{107}Pd–^{107}Ag chronometer. Such investigations showed that the troilites of IVA irons exhibit large (up to ~20%) excesses of radiogenic ^{107}Ag. These excesses were thought to be caused by the diffusion of radiogenic Ag from the metal phase (with very high Pd/Ag) to associated sulfide inclusions (with low Pd/Ag), either during slow cooling or secondary heating [4]. Such a scenario is realistic because metal fragments from IVA irons are known to display ^{107}Ag excesses of up to ~800% and these can dominate the composition of the sulfides. The isotopic systematics are different for Tl because radiogenic ingrowth did not generate such extreme variations in isotope compositions. The unradiogenic Tl isotope ratios of the troilites may thus reflect diffusion of Tl with preferential transport of the lighter ^{203}Tl isotope, as would be expected for kinetic isotope fractionation.

Using reasonable values for the relative abundances of Tl in sulfides and metal, it can be demonstrated that diffusion can generate troilites depleted in ^{205}Tl without significantly disturbing the isotope composition of co-existing metal. The proposed fractionation model can be tested, but this is difficult because this requires, for example, analyses of Tl diffusion profiles at metal – sulfide grain boundaries or the quantification of kinetic isotope fractionations for troilite – metal pairs using reasonable analog elements.

References: [1] Nielsen S.G. et al. 2006. *GCA*: in press. [2] Williams, H.M. et al. 2004. *Eos Trans. AGU* 85, F1251. [3] Quitte, G. et al. 2005. *Eos Trans. AGU* 86, Abstract P41E-02. [4] Chen, J.H. and Wasserburg, G.J. 1990. *GCA* 54: 1729–1743.

MILTON PALLASITE AND THE SOUTH BYRON IRON TRIO: A GROUPLET FORMED BY OXIDATION AND FRACTIONAL CRYSTALLIZATION.

V. S. Reynolds[1], T. J. McCoy[1], and W. F. McDonough[2]. [1]Department of Mineral Sciences, Smithsonian Institution, Washington, DC 20560-0119. [2]Department of Geology, University of Maryland, College Park, MD 20742.

Introduction: Among pallasites, only main group pallasites (PMG) show geochemical affinities to a group of irons (IIIAB), suggesting formation on the same parent body [1]. Additional links would greatly expand our understanding of core-mantle relationships. The Milton pallasite is ungrouped due to its high Ni and Ir concentrations, anomalous oxygen isotope signature, and FeO-rich olivine [2]. The metal composition of Milton is similar to the high-Ni irons South Byron, ILD 83500, and Babb's Mill (Troost's Iron), grouped as the South Byron trio [3]. We examined the metallographic structures and siderophile element abundances of these meteorites to determine whether they originated from the same parent asteroid and understand its formation.

Results: As high-Ni irons, the structures of all four are similar and dominated by plessite. South Byron and ILD 83500 contain sub-mm spindles of kamacite, as do larger plessitic areas of Milton. Rare sulfides and chromites are present, as are minute schreibersites that are associated with the kamacite spindles. The heat-treated Babb's Mill (Troost's Iron) lacks kamacite spindles. Milton also exhibits swathing kamacite surrounding silicates and oxides.

CI chondrite-normalized siderophile element patterns for Milton, South Byron and ILD 83500 are remarkably similar. Refractory siderophiles are enriched at ~10-100xCI. Volatile siderophiles exhibit smaller enrichments at ~1-10xCI. Milton and South Byron show depletions in elements readily oxidized (W, Mo, Fe, Cr, and P). Finally, as observed by [3], we show differences in platinum group elements (e.g., Re, Os, Ir) are consistent with fractional crystallization.

Discussion: The shared characteristics of Milton and the South Byron trio are consistent with formation on the same parent body, suggestive of a different history for these meteorites from other pallasite and high-Ni irons. In most high Ni irons (e.g., IVA, IVB, Tishomingo), high-T condensation had a significant role, forming a Ni-enriched, volatile-depleted siderophile element pattern [4, 5]. If condensation played a significant role in the formation of Milton-South Byron, these meteorites would be volatile siderophile depleted; however, they are not. While condensation processes may have a role in determining the bulk Ni concentration of this group, the uniform depletions of redox sensitive elements suggests that oxidation was a dominant process. We propose that oxidation controlled core formational processes on the parent body, as evidenced by the presence of Fe-rich silicates, chromite and phosphate [2]. Evidence for fractional crystallization is apparent in siderophile and PGE abundances, as suggested for the South Byron trio [3]. Unlike the pallasite in the PMG-IIIAB grouping [1], the pallasite in the Milton-South Byron grouplet appears to represent an early crystallizing solid.

References: [1] Mittlefehldt D.W. et al. *Planetary Materials.* [2] Jones R. H. et al. 2003. #1683. 34th LPSC [3] Wasson J. T. et al. 1989. *Geochimica et Cosmochimica Acta* 53, 735-744. [4] Corrigan C. M. and McCoy T. J. (2005) Oxygen in Asteroids and Meteorites, #7023. [5] Campbell A. J. and Humayun M. (2005) *Geochimica et Cosmochimica Acta* 69, 4733-4744.

MINERALOGY AND PETROLOGY OF THE MARE BASALT-RICH BRECCIA MET 01210.

K. Righter[1] and B. Bussey[2]. [1]NASA-JSC, Mailcode KT, 2101 NASA Parkway, Houston, TX 77058; kevin.righter-1@nasa.gov. [2]Planetary Exploration Group, Space Department, JHU/APL, 11100 Johns Hopkins Road, MP3-E169, Laurel, MD 20723.

Introduction: Meteorite Hills (MET) 01210 was announced as a 22.8 g anorthositic breccia, based on examination of one thin section [1]. Subsequent studies [2-6] have revealed the presence of many basaltic lithologies in addition to anorthositic. In some cases, basalt dominates by a 3:1 ratio (e.g., [4]). We have undertaken a petrographic study of MET 01210, and compare our results to other sections, thus giving a more comprehensive view of this interesting piece of the Moon.

Petrography and mineralogy: The section studied (,34) contains ten large clasts (> 500 μm), including five coarse-grained gabbros, two fine-grained feldspathic, two fine-grained basaltic (Fig. 1), and one symplectitic textured lithic clasts. Also present are numerous finer (< 500 μm) grained single mineral fragments, including many (5) large silica grains. Clasts make up approximately 15% of the mode, whereas the balance is made of either the finer mineral and lithic fragments and/or glassy matrix. Given this mixture of clast material and similar ratios apparent among the finer materials, this section also is consistent with a "mingled" breccia, as suggested by [6].

Discussion: The diverse clast types indicate an origin from a region that is proximal to both deep units such as the coarse grained gabbros and the fayalite-hedenbergite symplectites (also consistent with fine, extensive exsolution lamellae, [5]), and shallower units as the finer grained basaltic and anorthositic clasts. It is most similar in petrography to other mingled breccias such as Asuka 881757/Yamato 793169 (also noted by [3]).

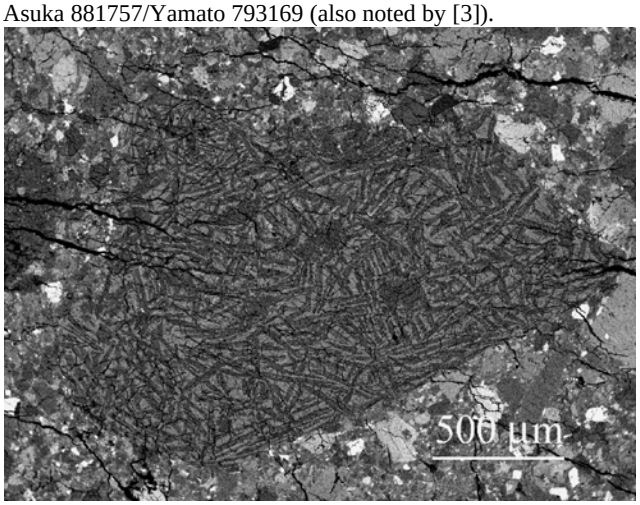

Figure 1: Melt clast containing laths of nearly pure anorthitic plagioclase (dark) in a glassy matrix of basaltic composition (lighter). Width is 2.0 mm.

References: [1] Satterwhite, et al. 2004. *Ant. Met. Newsl.*, 27(1). [2] Patchen A. D. et al. 2005. Abstract #1411. 36th Lunar & Planet. Sci. Conf. [3] Arai T. et al. 2005. Abstract #2361. 36th Lunar & Planet. Sci. Conf. [4] Zeigler R. A. et al. 2005. Abstract #2385. 36th Lunar & Planetary Planet. Sci. Conf. [5] Huber H. and Warren, P.H. 2005. Abstract #3512. 36th Lunar & Planet. Sci. Conf. [6] Korotev R.L. and Irving, A.J. 2005. Abstract #1220. 36th Lunar & Planet. Sci. Conf.

THE GREAT DIVERSITY OF PLANETARY MATERIALS RETURNED FROM THE QUEEN ALEXANDRA RANGE, ANTARCTICA.

K. Righter[1], R.P. Harvey[2], J. Schutt[2], C. Satterwhite[3], K.M. McBride[3], T.J. McCoy[4], and L. Welzenbach[4]. [1]NASA-JSC, Mailcode KT, 2101 NASA Parkway, Houston, TX 77058; kevin.righter-1@nasa.gov. [2]Dept. of Geology, Case Western Reserve University, Cleveland OH 44106-7216. [3]ESCG, Jacobs-Sverdrup, NASA-JSC, Houston, TX 77058. [4]Dept. Mineral Sci. NHB119, Smithsonian Institution, Washington DC, 20560.

Introduction: The Queen Alexandra Range (QUE) has yielded 3444 meteorites over six ANSMET collecting seasons. This huge number compares with 2186 from the Elephant Moraine, 1870 from Lewis Cliffs, 1600 from Allan Hills and 1130 from the Meteorite Hills regions. Although it is clear that many of the samples from this region are from a large ordinary chondrite fall, there is a great diversity of interesting samples.

Chondrites: Several chondrites found in the QUE range have contributed to the recognition of new chondrite groups. The metal-rich chondrites (QUE 94411, 94627 and 99309) are all now recognized to be part of the CB group [1]. Additionally, 9 CK chondrites have been found in the QUE region, and made a significant contribution to the great number of CK's overall that have come from Antarctica (~70%). QUE 97008 is recognized to be a rare low grade type 3 chondrite [2]. The region has also yielded 24 CM, 1 CO, 2 CR, 7 CV, 5 each of EH and EL chondrites.

Achondrites: A large range of valuable achondrites has come from this region, including three lunar meteorites (QUE 93069, 94269, and 94281), a shergottite (QUE 94201), 24 HED's, 3 ureilites, an ungrouped achondrite (QUE 93148), a winonaite (QUE 94535), and an unusual 2.4 kg ungrouped enstatite meteorite (QUE 94204 and seven paired masses from the 97 and 99 seasons). Two of the lunar meteorites are paired but are feldspathic regolith breccias [3], whereas the third (94281) is a glass-rich anorthositic-rich feldspathic regolith breccia [4]. These samples have provided new insight into the history and origin of the Moon. The 12 g basaltic shergottite is very unusual in that it is P-rich and contains up to 5% modal apatite, and as a result has provided age and petrologic information complementary to other shergottites [5]. The unusual achondrite QUE 93148 appears to be linked to pallasites [6]. The QUE region has also yielded 1 pallasite, 12 mesosiderites, and one enormous iron – 22 kg QUE 99001. The paucity of irons in Antarctica has been emphasized by [7], but this is a welcome anomaly.

Summary: The return of these samples, as well as the detailed studies that followed illustrates the potential of even a single Antarctic region to advance our knowledge and understanding of planetary materials.

References: [1] Weisberg, M.K. et al. 2001. MAPS 32, 401-418. [2] Grossman, J.N. and Brearley, A.J. 2005. MAPS 40, 87-122. [3] Korotev, R.L. et al. 1996. MAPS 31, 909-924. [4] Arai, T. and Warren, P.H. 1999. MAPS 34, 209-234. [5] McSween, H.Y. et al. 1996 GCA 60, 4563-4569. [6] Goodrich, C.A. and Righter, K. 2000. MAPS 35, 521-535. [7] Cassidy, W. 2003. Meteorites, Ice and Antarctica. Cambridge Univ. Press, 349 pp.

REVISITING THE DECOMPRESSED DENSITY OF MERCURY.

M. A. Riner[1,2], C. R. Bina[2] and M. S. Robinson[1,2]. [1]Center for Planetary Sciences, Northwestern University, Evanston, IL. E-mail: mariner@earth.northwestern.edu. [2]Dept. of Geological Sciences, Northwestern University, Evanston, IL.

Introduction: Mercury is unique among the terrestrial planets in terms of its low mass (3.302×10^{23} kg) and high average density (5.427 g/cc) that together imply an iron-rich composition relative to Venus, Earth, Mars and the Moon. Typically planetary bulk density is converted to decompressed density to allow meaningful interplanetary comparisons. The methodology used to calculate planetary decompressed density is not well documented in the scientific literature. Meaningful interpretations of decompressed density values require a clear elucidation of assumptions and methodology. In this abstract we present a detailed calculation of decompressed density for Mercury along with an analysis of the sensitivity of the method and implications for scientific interpretations of Mercury's decompressed density.

Method: The model uses a second-order Birch-Murnaghan equation of state to calculate Mercury's self compression, assuming an adiabatic temperature profile within the mantle and core [e.g. 1]. The temperature difference at the core mantle boundary is represented by the difference between the mantle and core adiabats extrapolated to zero pressure, ΔT_k. We assume a constant thermal expansion coefficient ($\alpha = 2.5\times10^{-5}$ K^{-1}).

The model is constrained by the observed total mass and total radius. Unfortunately the moment of inertia of Mercury is poorly constrained because Mercury rotates so slowly that non-hydrostatic contributions to the second degree gravitational potential coefficient, J_2, are larger than the hydrostatic contribution [e.g. 2]. The model was applied to 1300 random scenarios using the range of values shown in Table 1. The parameter values for the core are selected to cover a range of compositions (Fe and FeS) and phase (liquid and solid) [3].

	ρ_m^o g/cc	ρ_k^o g/cc	K_{Sm}^o GPa	K_{Sk}^o GPa	R_k km	Δ_{Tk} K
Values	3.35±0 .25	6.4± 1.4	180± 30	170± 40	2000 ±400	500± 500

Table 1 – From left to right the columns indicate the range of values for mantle density, core density, bulk moduli of mantle and core, (all at zero-pressure and 300K) core radius, and the temperature difference between the mantle and core adiabats extrapolated to zero pressure.

Results: Model scenarios with the lowest mass errors (± 10^{19} kg) have decompressed densities between 5.19 and 7.38 g/cc. The larger values for decompressed density correspond to larger core radii counterbalanced, to match the total mass, by low core densities, high core bulk moduli and/or hot core adiabats. Restricting the core radius to <2200km (rather than <2400km) results in decompressed density values between 5.19 and 6.38 g/cc.

Conclusions: Due to the uncertainty in the moment of inertia factor, core size, and the core and mantle density for Mercury, accurate calculation of the decompressed density is not possible at this time. Thus the commonly held assumption that, due to its small mass, the decompressed density of Mercury is well constrained at 5.3 g/cc is still open to question. However, application of this model to the Earth indicates that the decompressed density of the Earth is well constrained (±0.1 g/cc), even with variations in the mantle and core density and core size, as long as the total mass, total radius and moment of inertia factor constraints are met. Measurement of the moment of inertia for Mercury would better constrain the decompressed density.

References: [1] Stacey, F.D. 1992. Physics of the Earth. Brookfield Press [2] Ness, N.F. 1978. *Space Sci. Rev.* 21:527-553. [3] Harder H. and Shubert G. 2001. *Icarus* 151:118-122.

VARIATIONS IN LUNAR OPAQUE PHASE AND GRAIN SIZE: IMPLICATIONS FOR REMOTE SENSING OF TiO_2.

M.A. Riner[1], M.S. Robinson[1] P.G. Lucey[2], and D.S. Ebel[3]. [1]Center for Planetary Sciences, Northwestern University, Evanston, IL 60208. E-mail: mariner@earth.northwestern.edu. [2]Hawaii Institute of Geophysics and Planetology, SOEST, University of Hawaii, Honolulu. [3]American Museum of Natural History, New York, NY.

Introduction: Many workers have shown a correlation between visible color and TiO_2 abundance of lunar samples. However nagging uncertainties remain in the universal applicability of visible color differences to accurate prediction of TiO_2 abundance from remote sensing observations [e.g. 1,2]. Here we investigate two potentially important controls on UVVIS color of lunar soils that may hinder accurate TiO_2 estimates: presence of opaque mineralogy other than ilmenite, and opaque grain size variations.

Methods: Reflectance spectra of samples of powdered natural basalt, synthetic ilmenite ($FeTiO_3$) and synthetic ulvöspinel (Fe_2TiO_4) were measured (Ocean Optics HR2000CG-UV-NI, 200-1100nm at near zero phase angle (α) and/or RELAB 300-2800nm at α=30° [3]). Reflectance spectra of mixtures of these components were modeled using radiative transfer methods [4]. Preliminary assessment of the mixture modeling was confirmed by spectral measurements of four mixtures of ilmenite and basalt.

Results: The 415/750nm color ratio of ulvöspinel is 4% lower than ilmenite (Table 1), which reduces to < 1% in the modeled mixtures of the opaque minerals with basalt (Table 1). Some of the ratio change may be due to grain size distribution variations between the two samples. Decreasing the grain size of ilmenite from 20-63μm to <20μm decreases the 415/750 ratio by 9%.

Measured Samples	415/750	Modeled mixtures	415/750
Ilmenite (< 63 μm)	0.984	20% ilmenite	0.832
Ulvöspinel	0.947	40% ilmenite	0.865
Ilmenite (20-63μm)	1.020	20% ulvöspinel	0.829
Ilmenite (<20 μm)	0.931	40% ulvöspinel	0.857

Table 1. Relative color of measured mineral separates at varying grain sizes (α=0°), model mixtures from end-member spectra measured at α=30°.

Discussion: Ulvöspinel on the lunar surface is spectrally indistinguishable from ilmenite from the 415/750nm ratio alone. Since a given mass of ulvöspinel has one third less mass of TiO_2 than ilmenite, its occurrence results in a TiO_2 overestimate using this ratio. The change in the 415/750nm ratio caused by variations in the ilmenite grain size fractions considered here is twice as large as the difference between ulvöspinel and ilmenite (Table). Decreasing the grain size of a mineral (e.g ilmenite) in a mixture tends to increase its apparent abundance. Thus mixing systematics indicate that decreasing ilmenite grain size will increase the 415/750nm ratio while spectral changes have the opposite effect. The magnitude of these competing effects is unknown. The spectral changes due to particle size variation must, therefore, be considered in addition to the mixing systematics.

Conclusions: If some areas of the lunar regolith carry ulvöspinel as the dominant opaque mineral, estimates of TiO_2 abundance could be in error up to several weight percent. Spectral changes due to grain size variations in ilmenite affect the UVVIS ratio by ~9% for the size separates considered here. The effect on TiO_2 estimates also depends on the competing effect of mixing systematics. Actual variations in particle size distributions on the lunar surface may be smaller than those shown here, resulting in less dramatic variations in UVVIS ratio. Further work to assess the relative magnitudes of the competing effects of ilmenite grain size on UVVIS color is necessary.

References: [1] Elphic, R.C. et al. 2002. *JGR* 107: 10.1029/2000JE001460. [2] Gillis et al 2003. *JGR* 108:5009. [3] Pieters C.M. 1983. *JGR* 88:9534-9544. [4] Clark, B.E. et al. 2001 *MAPS* 31:1617-1637.

THE MOLECULAR STRUCTURE AND ISOTOPIC COMPOSITIONS OF THE INSOLUBLE ORGANIC MATTER IN CHONDRITES

F. Robert[1] and S. Derenne[2]. [(1)] LEME, CNRS-Muséum, Paris, France (robert@mnhn.fr) [(2)]LCBOP-BioEMCo, CNRS, ENSC, Paris, France.

The interstellar origin (ISM) of the Insoluble Organic Matter (IOM) extracted from CCs was originally supported by two independent observations: (1) its infrared spectrum mimics the interstellar spectrum around 3.3 microns [1] (2) its hydrogen is enriched in Deuterium relative to clay minerals [2]. To better constraint a model accounting for its organo-synthesis, the details of the molecular structure of the IOM were investigated since 1999. Several interesting discoveries have been made during the course of these studies involving pyrolysis GC-MS, MNR and Infrared spectroscopy, GC-iRMS and NanoSims imaging.

(1) The origin of the Universal 3.3 micron feature is now better understood: it results from the statistical distribution of C and H to form all the possible substitutions of the $-CH_2$ and $-CH_3$ bounds in aliphatic chains [3].

(2) The PAHs that constitute the largest moieties of fused benzene rings are formed by a number of cycles (3 on average in 2D), markedly lower than the PAHs detected in interstellar grains [4]. This may result from the photodissociation of the smaller aromatic units by UV radiations. This is most likely the signature of a protosolar process rather than ISM's.

(3) The benzene rings have a unique signature attesting of their extraterrestrial origin: they contain di-radilcoids [5]. Although predicted by quantum theory, these di-radilcoids were never observed in natural substances. As water circulation and/or parent body metamorphism would have erased these di-radicals, such a feature was likely established during the condensation of the IOM from the gas.

(4) Since no amine is present in the IOM (at a detection limit $\leq$7%), amino acids are not the by-products of the hydrolysis of a precursor polymer common to the soluble and the IOM [6].

(5) The planetary noble gases are mechanically trapped in the organic polymer and not in the benzenic molecules or in the left over oxides associated with acid extracts [7].

(6) The D/H ratios of the three main organic bounds (aliphatic, aromatic, benzylic) exhibit a systematic D enrichment in the weaker organic hydrogen bounds. Therefore, the enrichment in Deuterium was acquired after the formation of the IOM and, in this respect, IOM cannot be regarded as an interstellar heritage.

References:

[1] Ehrenfreund P., Robert F. and D'Hendecourt L. (1991) *Astron. Astrophys*., **252**, 712-717. [2] Robert F. and Epstein S. (1982) *Geochim. Cosmochim. Acta*, **16**, p. 81-95. [3] Gardinier A., Derenne S., Robert F., Behar F., Largeau C., and Maquet J. (2000) *Earth Planet. Sci. Lett*. **184**, 9-21. [4] Derenne S., Rouzaud J-N, Clinard C. and Robert F. (2005) *Geochim. Cosmochim. Acta*, **69**, No. 15, 3911-3918. [5] Binet L., Gourie D., Derenne S., Robert F. and Ciofini I. (2004). *Geochim. Cosmochim. Acta* **68**, 881-891. [6] Remusat L., Derenne S., Robert F. and Knicker H. (2005) *Geochim. Cosmochim. Acta*, **69**, No. 15, pp. 3919–3932. [7] Marrocchi Y., Derenne S., Marty B and Robert F. *Earth Planet. Sci. Lett*. **236**, No. 3-4, 569-578. [8] Remusat et al., (2006) *Earth Planet. Sci. Lett* **243**, 15-25.

A CATALOGUE OF LARGE METEORITE SPECIMENS FROM CAMPO DEL CIELO METEORITE SHOWER, CHACO PROVINCE , ARGENTINA.

M. C. L. Rocca , Mendoza 2779-16A, Ciudad de Buenos Aires, Argentina, (1428DKU), maxrocca@hotmail.com.

Introduction: The Campo del Cielo meteorite field in Chaco Province, Argentina, (S 27º 30', W 61 º42') consists, at least, of 20 meteorite craters with an age of about 4000 years.

The area is composed of sandy-clay sediments of Quaternary-recent age. The impactor was an Iron-Nickel Apollo-type asteroid (Octahedrite meteorite type IA) and plenty of meteorite specimens survived the impact. Impactor's diameter is estimated 5 to 20 meters. The impactor came from the SW and entered into the Earth's atmosphere in a low angle of about 9º. As a consequence , the asteroid broke in many pieces before creating the craters. The first meteorite specimens were discovered during the time of the Spanish colonization. Craters and meteorite fragments are widespread in an oval area of 18.5 x 3 km (SW-NE), thus Campo del Cielo is one of the largest meteorite's crater fields known in the world.

Crater nº 3, called "Laguna Negra" is the largest (diameter: 115 meters). Inside crater nº 10, called "Gómez", (diameter about 25 m.), a huge meteorite specimen called "El Chaco", of 37,4 Tons, was found in 1980. Inside crater nº 9, called "La Perdida" (diameter : 25 x 35 m.) several meteorite pieces were discovered weighing in total about 5200 kg.

The following is a catalogue of large meteorite specimens (more than 200 Kg.) from this area as 2005. Information given is the name of the meteorite, its weight and date of discovery and its current location.

References: [1] EL ABIPON: 460 Kg.- 1936-Museo Argentino de Ciencias Naturales,(MACN), Buenos Aires city, Argentina. [2] EL CHACO: 37,4 Tons -1980-Gancedo , Chaco, Argentina. This specimen is the second heaviest meteorite known in the World. [3] EL MATACO: 998 Kg.-1937- Museo Provincial, Rosario, Santa Fe, Argentina. [4] EL MOCOVI: 732 Kg.-1925-MACN, Buenos Aires city, Argentina. [5] EL PATIO: 350 Kg.-Found before 1960-Estancia El Taco, Chaco, Argentina. [6] EL TACO: 1998 Kg.-1962-Main mass at National Museum of Natural History, Smithsonian Institution, Washington ,DC; USA; 600 Kg. at Planetarium of Buenos Aires city, Argentina. [7] EL TOBA: 4210 Kg.-1923-MACN, Buenos Aires city, Argentina. [8] EL TONOCOTE: 850 Kg.-1931-Planetarium, Buenos Aires city, Argentina. [9] LA PERDIDA(1): 1625 Kg.-1965- Planetarium, Buenos Aires city, Argentina. [10] LA PERDIDA(2): 3370 Kg.-1965-Still in the crater. [11] MESON DE FIERRO: 15 Tons – 1576 – Lost. [12] RUNA POCITO: 750 Kg.-1803- British Museum, London, United Kingdom. [13] NO NAME: 10 Tons.-1997-Near its find site, Chaco, Argentina. [14] LA SORPRESA: 7-10 Tons-2005-Still in the crater .

Acknowledgements: This work was funded by The Planetary Society, Pasadena, California, USA.

TWO NEW POTENTIAL METEORITE IMPACT SITES IN CHUBUT PROVINCE , ARGENTINA.

M. C. L. Rocca , Mendoza 2779-16A, Ciudad de Buenos Aires, Argentina, (1428DKU), maxrocca@hotmail.com.

Introduction: **Site One**: A remarkable site of a possible new large meteorite impact craters field has been studied by the examination of Landsat and aerial photographs (Instituto Geografico Militar).

More than 100 small possible simple-type craters are widespread over an area of 27 × 15 Km. located at Meseta Filu-Co, Bajada del Diablo, Chubut Province, Argentina (42º45'S 67º30'W). Largest crater's diameter is 1 Km.. Most of these craters show clear evidences of having raised rims. Fourteen craters have diameters between 300 and 1000 meters.

Craters are mainly located on areas were fluvial sedimentary deposits (conglomerates) of Tertiary and Quaternary age are exposed but, many craters are also located on several different geologic terrains like, e.g., small basaltic plateaux and piroclastic rocks.

Areas exposing Recent fluvial sediments show no crater so the impact event was not very recent [1]. No doubt, many craters have been erased by the Recent fluvial erosion processes and what we see today is just a fraction of the original population of craters.

When meteorite showers reach the ground they distribute themselves into a strewn field which usually defines an elliptical shaped area called, the dispersion ellipse. The long axis is coincident with the direction of motion of the swarm and the most massive fragments normally fall at the far end of the dispersion ellipse [2].

There is no evidence for those patterns in the case of Bajada del Diablo craters. Medium to large craters are randomly distributed all over the whole area of the craters field. No clear dispersion ellipse is visible in the images.

Most probably, this craters field is the result of the impact of a 100 to 200 meters wide rubble-pile type asteroid which was broken in hundreds of fragments by the Earth's gravity force short before entering into the atmosphere. Then the swarm of fragments created the crater field..

Site two: Meseta del Canguel, Chubut Province, (44º28'S 68º35'W).

Three possible simple-type impact craters located in an Y-shape configuration on a olivine-basalt plateau. Craters show raised rims.

Diameters: 1.3, 0.8 and 0.6 Kilometres.

Age is estimated in less than 20 Ma [3]

Acknowledgements: This work was funded by The Planetary Society, Pasadena, CA, USA.

References: [1] Corbella H. (1987), Revista Asociación Mineralogia, Petrología y Sedimentologia 18 (1/4), p. 67 (in Spanish). [2] Krinov E. (1966), Giant Meteorites, Pargamon Press, New York. [3] Ardolino A. et al. (1999) Anales SEGEMAR 29,(1): 579-612.

MAGNETIC CLASSIFICATION, WEATHERING AND TERRESTRIAL AGES OF ANTARCTIC ORDINARY CHONDRITES.

P. Rochette[1], L. Folco[2] J. Gattacceca[1], C. Berteloot[1], and C. Suavet[1]. [1]CEREGE University of Aix-Marseille 3, France. [2]Museo Nazionale Antartide Siena Italy

Magnetic susceptibility (χprovides a means to discriminate rapidly between LL, L and H falls [1] . This method allows rapid scan of collections without sample preparation and with portable instruments [2] However, the classification abilities are hampered by weathering: for example a weathered H chondrite can yield the same susceptibility as a fresh L chondrite. The three well separated Gaussian distributions for fresh LL, L and H [1] are skewed and partially merged by the weathering effect. The use of density measurements [3] does not really help to solve the ambiguity. In order to delineate this effect, we propose a simple mathematical model using the logχ versus terrestrial age function as input data. To constrain the model logχ versus terrestrial age function, we can use meteorites with cosmogenic isotopes derived ages. We will present data on Antarctic meteorites (from PNRA and ANSMET collections), showing a rather significant correlation for H and L, at odds with the literature contention that terrestrial age is independent of weathering grade in Antarctic meteorites. This contradiction likely arises from the fact that the weathering grade adopted for Antarctic meteorites (WG) is a sort of color color index, that does not represent correctly the amount of metal oxidized in non-magnetic phase (akagaenite, goethite, paramagnetic Fe^{3+}), which is actually what logχ measures. We will discuss the dispersion observed in the correlation in terms of uncertainties in terrestrial age and log determination, as well as in terms of different weathering processes depending on the story of the meteorite on or in the ice. As a perspective the calibration curve can be used to predict the terrestrial age distribution of a given collection for which logχ measurements are available.

References: [1] Rochette, P., et al.., 2003 *Meteoritics & Planetary Science* 38, 251-268. [2] Folco, L. et al., 2006, *Meteoritics and Planetary Sciences* 41, 343–353. [3] Consolmagno G. J. et al., 2006, *Meteoritics and Planetary Sciences* 41, 331-342.

MAGNETIC CLASSIFICATION OF C, E, K, R AND UNGROUPED CHONDRITES.

P. Rochette[1], J. Gattacceca[1], L. Sagnotti[2], L. Folco[3] G. Consolmagno[4] and M. Denise[5]. [1]CEREGE CNRS University of Aix-Marseille 3, France. [2]INGV Roma, Italy [3]Museo Nazionale Antartide Siena Italy, [4]Specola Vaticana, Vatican City, [5]MNHN Paris.

Magnetic susceptibility (χprovides a mean to discriminate rapidly between LL, L and H falls [1] . We expand this work to C, E, K, R and ungrouped chondrites, based on previously published database [2,3] and new data. The complete database corresponds to more than 400 different meteorites (and 700 samples) from 21 large collections around the world. A preliminary summary was included in [4]. Once weathering effect is isolated (mostly visible for metal rich material: E, CR, CH), most groups, except CM and CV, yield well grouped logχ values, indicative of a rather restricted variation of the amount of magnetic minerals (metal, magnetite or pyrrhotite).

One can distinguish 3 categories: weakly magnetic R (mean logχ of 3.2), moderately magnetic CO, K, CK, CI (logχ from 4.5 to 4.9, i.e. similar to L) and strongly magnetic CR, CH and E (logχ from 5.1 to 5.4, i.e. similar to H). On the other hand a wide range of values are observed for CM and CV, from 3.3 to 4.9, i.e. a factor 40 range in magnetic mineral amount (wt%), while the total iron amount is much less variable. No tendency for a grouping toward a specific value is observed, although one may distinguish a “grouplet” of strongly magnetic CM, already pointed out as anomalous: Bells, Essebi, Niger, MAC02606, MET01177. The corresponding range of redox conditions encountered in CM and CV should be discussed in terms of metamorphism on the parent bodies, but it seems that larger values (near 4.9) are observed for less metamorphosed meteorites. This large range allows to propose pairing hypothesis for Antarctic CV and CM. Among the ungrouped C2 to C4 a somewhat similar range is observed although a tendency toward values near 4.9 (case of e.g. Tagish Lake, Coolidge) is somehow visible.

Other ungrouped, anomalous meteorites are tentatively compared to some groups based on their logχ value. For example Kaidun fits with an average CI magnetic content, Taffafaset with a CR magnetic content.

References: [1] Rochette, P., et al.., 2003 *Meteoritics & Planetary Science*., 38, 251-268. [2] Rochette et al., 2001, Quaderni di Geofisica [3] Smith et al., 2006, *Meteoritics and Planetary Sciences* 41, 355-374 [4] Folco, L.et al., 2006, *Meteoritics and Planetary Sciences* 41, 343–353.

SRTM INVESTIGATION OF THE ARAGUAINHA IMPACT CRATER, CENTRAL BRAZIL.

R. Romano[1], G. R. Cooper[2], W. U. Reimold[2,3]. [1]Department of Geology, Federal University of Ouro Preto, Minas Gerais, 35400-000 Brazil. E-mail: rcromano@gmail.com. [2]Impact Cratering Research Group, School of Geosciences, Univ. Witwatersrand, Johannesburg, RSA. [3]Museum für Naturkunde (Mineralogie), Humboldt-Universität, Berlin, Germany.

The 40 km diameter Araguainha impact structure (at 16 47' S: 52 59' W) was excavated ca. 245 Ma ago in flat-lying Permian to Devonian sediments of the intracratonic Paraná Basin, central Brazil. The impact origin for the structure is based on the presence of shatter cones and bona fide shock deformation of minerals from throughout the central parts of the structure. The structure is characterized by an ~8-km-wide central uplift surrounded by a 10-15 km wide zone of annular rings formed by vertical and lateral movements of the target rocks during the collapse stage [1].

In this study we analyzed 3 arc second Shuttle Radar Topography Mission (SRTM) data and enhanced thematic Mapper (ETM+) Landsat images for the region around Araguainha. Several enhancement methods for circular structures were applied to the SRTM data, such as radial sunshading [2].

Color composite Landsat ETM+ with RGB 7-4-2 bands, sharpened with the panchromatic band, shows a structure comprising a 6 km wide, near-circular central uplift, open to the southeast, surrounded by an apparently flattish depression of about 5 km width, with a ca. 7.5 km radius intermediate ring feature, followed by the outer rim at 20-22 km from the center. The structure appears to be very well preserved in the N and NW sectors, where it was not affected by erosion by the Araguaia River, which cuts the structure across the SW and NE sectors.

The SRTM raw data for the area of the structure provide a detailed representation of the annular and concentric drainage pattern. The sunshading filters provide a much clearer image of the structure than the Landsat imagery. As in the Landsat image, the SRTM data show a structure with prominent annular rings in the N and NW sectors. The radial average filter applied gives more detail about the ring features. A central topographic low is observed with a radius of 2.1 km, followed by an outer central ring of 3.6 km and an annular trough of ca. 3.4 km radius. The first intermediate ring appears as a narrow feature at 7 km. The second intermediate ring, at 12.2 km, is the most prominent one, with an average elevation of 100 m compared to the annular trough. A third intermediate ring appears at 14.6 km from the center, followed by the outer rim at 18.5 km.

The Landsat and SRTM data provide a powerful tool for detailed observations of structure and morphology of impact structures. These data indicate that the Araguainha Structure comprises a complex peak-ring structure. Comparing these features with other similar impact structures on Earth could provide fundamental information with regard to the identification of such structures and for the understanding of cratering mechanisms.

References: [1] Lana et al. 2006. *Geology* 34(1):9-12; [2] Cooper, G. R. J. 2003. *Computers & Geosciences* 29:941-948.

THE NATURE OF THE LITHIUM-RICH PHASE FOUND IN MIL 03346 MESOSTASIS.

D. Rost[1], E. P. Vicenzi[1], M. Fries[2], and A. Steele[2]. [1]Smithsonian Institution, Dept. of Mineral Sciences, Washington, D.C. 20560, USA. E-mail: rostd@si.edu. [2]Geophysical Laboratory, Carnegie Institution of Washington, Washington, D.C. 20015, USA.

Introduction: Martian meteorite MIL 03346 putatively originates from an upper stratum of the nakhlitic lava flow(s) [1]. The recent discovery of Li-rich grains in its mesostasis [2] is important for understanding the preterrestrial aqueous alteration processes in nakhlites, since a readily dissolvable Li host phase is a likely source for the Li enriched in secondary clay minerals found in Nakhla and Lafayette [3,4] – by way of percolating fluids. Here we present additional spectroscopic information regarding the nature of the Li-enriched phase in MIL 03346.

Methods: Polished thin sections were used for ToF-SIMS analyses (IONTOF TOF-SIMS IV), confocal Raman examination (WITec α-SNOM), and EDX measurements (Thermo Electron NSS on both a JEOL 840A and an FEI Nova NanoSEM 600).

Results: The MIL 03346 mesostasis contains small grains (10–50 µm) with compositions that suggest fayalite, *i.e.*, ~$(Fe_{0.91}Mg_{0.06}Mn_{0.03})_2SiO_4$ if cast into the olivine formula, and high Li contents ranging from 44 to 100 ppm. However, Raman spectroscopic analysis identified fayalite only in the cores of a few grains. The majority of the grains are not olivine as their distinctive Raman spectrum is incompatible with common mafic silicates, *e.g.*, olivine and pyroxene. The Li concentrations in both phases are indistinguishable. A ~50 µm thick rim of phenocristic olivine in contact with the mesostasis turned out to be this unknown phase as well, and is similarly rich in Li.

Small deviations in the composition of the unknown phase relative to the fayalite (Fe depletion and O enrichment) suggest the ferriolivine laihunite, $Fe^{2+}Fe^{3+}{}_2(SiO_4)_2$. This is supported by similar Raman spectra taken from our National Museum of Natural History's laihunite mineral specimen.

Discussion: Oxidizing conditions and temperatures of ~700°C convert olivine (fayalite) into ferriolivine (laihunite) and other reaction products, *e.g.*, hematite and magnesioferrite [5–7]. In MIL 03346, no such additional oxides have been observed in connection with the assumed laihunite. Therefore, it is difficult to speculate on the conditions of laihunitization in MIL 03346.

The high Li concentrations might be the result of a general trend of Li enrichment in the nakhlitic parental melt as it is also documented in increasing bulk meteorite contents of Li (see overview in [2]) at supposed shallower stratigraphic levels [8,1]: Eventually, the olivine in the MIL 03346 mesostasis was the least unsuitable phase to incorporate Li.

The Li concentrations in these grains are comparable to those in secondary clays [3,4] and could represent the original siting of Li, before it was mobilized by penetrating fluids.

Outlook: Analyses of other laihunite samples are planed to corroborate its presence in MIL 03346. EMPA will be employed to confirm our current microanalytical observations.

References: [1] Mikouchi T. et al. 2005. *LPS XXXVI* #1944. [2] Rost D. et al. 2006. *LPS XXXVII* #2362. [3] Rost D. and Vicenzi E. P. 2004. *Meteoritics & Planetary Science* 39:A92. [4] Rost D. et al. 2005. *LPS XXXVI*:#2306. [5] Kondoh S. et al. 1985. *American Mineralogist* 70:737–746. [6] Iishi K et al. 1997. *Physics and Chemistry of Minerals* 25:8–14 [7] Khisina N. R. et al. 1998. *European Jornal of Mineralogy* 10:229–238. [8] Mikouchi T. et al. 2003. *LPSC XXXIV* #1883

OXIDATION STATE AND O-ISOTOPIC COMPOSITIONS OF EQUILIBRATED H CHONDRITES.

Alan E. Rubin, Institute of Geophysics, University of California, Los Angeles, CA 90095-1567, USA; aerubin@ucla.edu.

Equilibrated members of the H-L-LL sequence show a correlation between mean group oxidation state (as represented by olivine Fa) and mean group O-isotopic composition (indicated by $\Delta^{17}O$): H4-6 (Fa 18.8 mol%, $\Delta^{17}O$ = 0.73‰), L4-6 (Fa 24.7 mol%, $\Delta^{17}O$ = 1.07‰), LL4-6 (Fa 29.4 mol%, $\Delta^{17}O$ = 1.26‰) [1,2]. The correlation is not restricted to the group means, but also occurs among 14 H-chondrite falls [3]. I have analyzed olivine in six additional H4-6 falls for which O-isotopic compositions were previously determined [2]: Ambapur Nagla, H5 (Fa 18.2±0.1, n=28; $\Delta^{17}O$ = 0.75‰); Charsonville, H6 (Fa 17.6±0.2, n=22; $\Delta^{17}O$ = 0.65‰); Forest City, H5 (Fa 18.0±0.2, n=27; $\Delta^{17}O$ = 0.75‰); Kernouvé, H6 (Fa 18.6±0.2, n=26; $\Delta^{17}O$ = 0.78‰); Pantar, H5 (Fa 18.3±0.5, n=27; $\Delta^{17}O$ = 0.56‰); Weston, H4 (Fa 18.3±0.3, n=23; $\Delta^{17}O$ = 0.88‰). [At this point, 20 of the 22 H-chondrite falls for which O-isotopic data are available have been analyzed; electron microprobe analyses of the two remaining H chondrites (H5 Leighton and H6 Cape Girardeau) are pending.] The correlation between olivine Fa and $\Delta^{17}O$ is significant: $r = 0.574$, $n = 20$, $2\alpha = 0.008$, significant at the 99.2% confidence level. However, three samples (Pantar, Weston, Tysnes Island) are solar-gas-rich regolith breccias; the first two of these are outliers. Because regolith breccias contain exotic clasts of different chondrite groups [4,5], their bulk O-isotopic compositions are not representative of pristine H-chondrite material. If these breccias are omitted from the correlation, its significance increases: $r = 0.725$, $n = 17$, $2\alpha = 0.001$, 99.9% confidence level.

There are also correlations between olivine Fa and $\Delta^{17}O$ among H-chondrite falls of the same petrologic type (again omitting the regolith breccias): H5 ($r = 0.825$, $n = 5$, $2\alpha = 0.09$, 91% confidence level); H6 ($r = 0.832$, $n = 7$, $2\alpha = 0.02$, 98% confidence level). However, the H4 correlation is not significant: $r = 0.569$, $n = 5$, $2\alpha = 0.36$, 64% confidence level.

It is likely that the correlations between oxidation state and O-isotopic composition in OC were established in the solar nebula. Rubin [3] proposed that a single component (^{17}O-rich phyllosilicate) was acquired by OC during agglomeration; H chondrites acquired the lowest abundance and became the most reduced OC with the lightest O isotopes. Different amounts of this component were incorporated into individual batches of H-chondrite material irrespective of their future parent-body thermal histories.

Equilibrated L- and LL-chondrite falls show no intragroup correlations between Fa and $\Delta^{17}O$ [3]; the appreciable scatter in the L data and even greater scatter in the LL data may be caused by the presence in these rocks of an additional, heterogeneously distributed, O-bearing component that is more abundant in LL chondrites. One candidate is the set of coarse silica-rich clasts in LL3.6 Parnallee that have $\Delta^{17}O$ values of 1.5 to 3.0‰ [6]. Even during metamorphism to petrologic-type-6 levels, these clasts would not have completely equilibrated their O isotopes [7].

References: [1] Rubin A.E. 1990. *Geochim. Cosmochim. Acta* 54:1217-1232. [2] Clayton R.N. et al. 1991. *Geochim. Cosmochim. Acta* 55:2317-2337. [3] Rubin A.E. 2005. *Geochim. Cosmochim. Acta* 69:4907-4918. [4] Noonan A.F. and Nelen J.A. 1976. *Meteoritics* 11:111-130. [5] Keil K. and Fodor R.V. 1980. *Chem. Erde* 39:1-26. [6] Bridges J.C. et al. 1995. *Meteoritics* 30:715-727. [7] Olsen E.J. et al. 1981. *Earth Planet. Sci. Lett.* 56:82-88.

SHOCK AND ANNEALING IN EL CHONDRITES.
Alan E. Rubin, Institute of Geophysics, University of California, Los Angeles, CA 90095-1567, USA; aerubin@ucla.edu.

Shock has affected the structure, texture and mineralogy of EL chondrites of all petrologic types. **EL3**: Shock stages range from S2-S5; many samples are foliated. Impact deformation caused foliations in OC [1]; it is likely that EL3 foliations also formed by impact. Extensive shock melting is precluded by the presence of excess ^{53}Cr in EL3 sphalerite [2]. **EL4**: The three rocks I studied are impact-melt breccias (IMBs) of shock-stage S2. QUE 94368 contains euhedral enstatite grains protruding into kamacite and euhedral graphite laths surrounded by metal and silicate; these features are characteristic of enstatite-chondrite IMBs (e.g., EH Abee [3]). QUE94368 contains euhedral grains of sinoite (Si_2N_2O) that probably crystallized from the melt [4]. Grein 002, which was partly impact melted, contains euhedral grains of enstatite, graphite and sinoite [5]. MAC02747 contains euhedral grains of enstatite and graphite. **EL5-EL6**: Nearly all of these rocks are S2, but many EL6 chondrites have features suggesting much higher shock levels at an earlier period. Blithfield is a chondrule-free IMB with large sulfide-rich, kamacite-poor clasts, a metal-rich matrix, and cm-size metal veins. Hvittis is a fragmental breccia with impact-melt-rock clasts. Atlanta contains a sulfide-rich, kamacite-poor clast and cm-long metal veins. NWA 2213 has euhedral grains of enstatite and graphite, kamacite grains with small troilite blebs, and troilite grains with small kamacite blebs. Forrest 033, GRO95626 and QUE97462 contain euhedral grains of enstatite and graphite. Other EL6 chondrites also contain euhedral enstatite grains. Euhedral grains of sinoite occur in Forrest 033, Hvittis, Jajh deh Kot Lalu, Pillistfer, Ufana, Yilmia, ALHA81021, LEW88714, EET90102 and Neuschwanstein. Diopside is present in EL3 MAC88136 [6], EL4 Grein 002 [5], EL6 EET90102 [7] and EL6 NWA 2213. Diopside is probably a primary phase in EL3 chondrites. In EL4-6 chondrites, diopside may have formed by reaction of oldhamite and enstatite at high temperatures followed by quenching [7]. The brecciated and melted textures of some EL6 chondrites and textural and mineralogical similarities to the impact-melted portions of EL4 chondrites (including the presence of sinoite, diopside, euhedral enstatite and euhedral graphite) suggest that at least some EL6 chondrites are annealed IMBs. The EL4-6 chondrites may have formed from EL3 chondrites by variable degrees of impact heating, burial beneath insulating regolith material, and annealing. Annealing in the EL4-6 chondrites erased shock effects in pyroxene, producing grains with sharp optical extinction. Subsequent impacts caused undulose extinction to develop in pyroxene, changing the rocks' shock-classifications to stage S2. It is unclear to what extent the decay of short-lived radionuclides contributed to EL-chondrite metamorphism. About 60% of EL6 chondrites have similar ^{21}Ne CRE ages (27±6 Ma) [8,9] suggesting that these rocks were in the same location on their parent asteroid and likely experienced similar shock and thermal histories.

References: [1] Sneyd D.S. et al. 1988. *Meteoritics* 23:139-149. [2] El Goresy A. et al. 1992. *Lunar Planet. Sci.* 23:331-332. [3] Rubin A.E. and Scott E.R.D. 1997. *Geochim. Cosmochim. Acta* 61:425-435. [4] Rubin A.E. 1997. *Am. Mineral.* 82:1001-1006. [5] Patzer A. et al. 2004. *Meteorit. Planet. Sci.* 39:1555-1575. [6] Lin Y.T. et al. 1991. *Lunar Planet. Sci.* 22:811-812. [7] Fogel R.A. 1997. *Meteorit. Planet. Sci.* 32:577-591. [8] Crabb J. and Anders E. 1981. *Geochim. Cosmochim. Acta* 45:2443-2464. [9] Patzer A. and Schultz L. 2001. *Meteorit. Planet. Sci.* 36:947-961.

Al-26 IN SEMARKONA (LL3.0) CHONDRULES: ONSET AND DURATION OF CHONDRULE FORMATION. N. G. Rudraswami[1], B. K. Chattopadhyay[2], B. K. Bandopadhyay[2] and J. N. Goswami[1], [1]Physical Research Laboratory, Ahmedabad – 380009, India, [2]Geological Survey of India, Kolkota – 700016, India. (E-mail: gowda@prl.res.in).

Al-Mg isotope records have been studied in Semarkona (LL3.0) chondrules to further our understanding of the onset and duration of chondrule formation. The extremely low degree of thermal metamorphism suffered by this meteorite in its parent body is expected to preserve the pristine records of Al-Mg isotope system in the analyzed chondrules. An earlier study of ^{26}Al records in Semarkona chondrules [1] suggested onset of chondrule formation about 2 Ma after CAI and a short duration of chondrule formation. Studies of chondrules from other UOCs support late formation of chondrules but argue for an extended duration of chondrule formation of >2 Ma [2-4].

A polished thin section of Semarkona was mapped using SEM and EPMA to identify chondrules containing Al-rich phases (glassy mesostasis and rare plagioclase). A Cameca ims-4f ion microprobe was used for isotopic studies of a dozen selected chondrules. The presence of Mg-rich microcrystallites within the Al-rich glassy phases makes it difficult to carry out meaningful isotopic study in many chondrules. However, we could detect well resolved ^{26}Mg excess (from ^{26}Al decay) in four of the chondrules where we could conduct meaningful isotopic analysis. The data yielded well-behaved isochrones and we infer initial ^{26}Al/^{27}Al ratio of $(1.24\pm0.26)\times10^{-5}$, $(1.14\pm0.27)\times10^{-5}$, $(1.10\pm0.12)\times10^{-5}$ and $(5.4\pm0.2)\times10^{-6}$, respectively, for these chondrules.

The initial ^{26}Al/^{27}Al values obtained in this study reinforce the suggestion that formation of CAIs preceded chondrules formation by at least 1.5 Ma. Further, three of the chondrules have very similar initial ^{26}Al/^{27}Al that suggests a short duration of chondrule formation in the early solar system. However, the fourth chondrule, that has a large spread in Al/Mg ratio and a very well behaved Al-Mg isotope systematic, has an initial ^{26}Al/^{27}Al ratio lower than the other chondrules. Low initial ^{26}Al/^{27}Al ratios of (4 to 8) $\times10^{-6}$ have also been reported earlier [5] for Semarkona and Bishunpur (LL3.1) chondrules. These data argue for an extended duration of chondrule formation unless we invoke thermal metamorphism of these chondrules in a pre-parent body setting. Both the proposition of an extended duration of chondrule formation and thermal metamorphism in a pre-parent body environment require isolation of CAIs and chondrules for significant durations of more than 3 Ma before their mixing and accretion to form the chondritic parent bodies. This is in contrast to the fact that accretion, differentiation and crust formation in the case of parent bodies of differentiated meteorite was complete within 3-5 Ma following the formation of CAIs [see, e.g., 6-9].

References: [1] Kita N.T. et al. 2000. *GCA* 64:3913–3922. [2] Russell S.S. et al. 1996. *Science* 273:757-762. [3] Huss G.R et al. 2001. *MAPS* 36:975–997. [4] Mostefaoui S. et al. 2002. *MAPS* 37:421-438. [5] McKeegan K. et al. 2000. Abstract # 2009, 31st LPSC. [6] Srinivasan G. et al. 1999. *Science* 284: 1348-1350. [7] Kleine et al. 2002. *Nature* 418: 952-955. [8]Yin Q et al. 2002. *Nature* 418: 949-952. [9] Kleine et al. 2005. *GCA* 69: 5805-5818.

NWA 2999 AND OTHER ANGRITES: NO COMPELLING EVIDENCE FOR A MERCURIAN ORIGIN.

A. Ruzicka and M. Hutson. Cascadia Meteorite Laboratory, Dept. of Geology, Portland State University, 17 Cramer Hall, 1721 SW Broadway, Portland, OR 97207.

Introduction: NWA 2999 is the tenth known angrite, and contains disequilibrium textural features which recently led to the suggestion that it and other angrites were derived from Mercury [1,2]. These features include diopsidic-augitic clinopyroxene (*cpx*) + spinel (*sp*) symplectites around plagioclase (*plag*), and discontinuous coronas of *plag* around *sp*. The textures were interpreted by Irving et al. [1,2] as having formed by crossing the olivine (*ol*) + *plag* = *sp* + orthopyroxene (*opx*) + *cpx* reaction boundary twice, with the symplectites forming by transition to higher pressure (>6.7 kb), and the *plag* coronas forming upon pressure release. We suggest instead that these textures were more likely produced during low pressure crystallization.

Melting and crystallization in angrite systems: Partial melts of carbonaceous chondrite precursors under relatively oxidizing conditions at 1 bar produce angrite-like melt compositions and mineralogies [3,4]. The low-pressure liquidus phase diagrams of Longhi [4] show that *sp* and *plag* can either appear or disappear as temperature is changed under relatively oxidizing conditions. For an Allende (CV3) oxidized composition with no Fe removed, initial melting begins at ~1130 ºC with co-existing *ol*, *cpx*, and *sp*. *Plag* forms and *cpx* disappears after ~4% melting at ~1162 ºC and *plag* disappears after 19% melting at ~1248 ºC. For an Allende composition with 10% Fe removed, *ol* + *cpx* + *plag* + *sp* coexist with the first melt, *sp* disappears after ~1% melting, *cpx* disappears after ~1.7% melting at ~1166 ºC, and after 22% melting *plag* disappears and *sp* reappears. We suggest that *plag* coronas around *sp* in NWA 2999 formed as temperature dropped to ~1250 ºC when *plag* began to crystallize. *Cpx* + *sp* symplectites around *plag* probably formed as temperature dropped to ~1165 ºC, when both *cpx* and *sp* were stable. Thus, cooling during crystallization can explain the disequilibrium textures. Pressure changes and large planetary bodies are not required.

Angrites from Mercury? In contrast to Irving and coworkers [1,2], we find no compelling evidence that angrites were derived from Mercury. Arguments against a mercurian origin for angrites were given previously [5] and include their old crystallization ages (4.56 Ga) and ferrous compositions. In particular, the ferrous compositions and reflectance spectra of angrites are completely at odds with spectral data for Mercury [6,7]. The minimal shock and metamorphic effects experienced by most angrites are also inconsistent with their derivation from a large body [8]. Finally, NWA 2999 contains ~8% metal [2], unlike what one would expect for Mercury's crust or mantle.

References: [1] Irving T. et al. (2005) *Eos Trans. AGU* 86 (52). [2] Kuehner S.M et al. (2006) *LPS XXXVII*, #1344. [3] Jurewicz A. et al. (1993) *Geochim. Cosmochim. Acta* 57, 2123-2139. [4] Longhi J. (1999) *Geochim. Cosmochim. Acta* 63, 573-585. [5] Love S. and Keil K. (1995) *Meteoritics* 30, 269-278. [6] Burbine T. et al. (2002) *Meteorit. Planet. Sci.* 37, 1233-1244. [7] Burbine T. et al. (2001) *LPS XXXII*, #1857. [8] Mittlefehldt D. et al. (2002) *Meteorit. Planet. Sci.* 37, 345-369.

TRACE ELEMENT COMPOSITIONS OF NORMAL, DUSTY, AND CLEAR OLIVINE IN CHAINPUR CHONDRULES.

A. Ruzicka[1] , C. Floss[2], and M. Hutson[1] [1]Dept. Geology, 17 Cramer Hall, 1721 SW Broadway, Portland State University, Portland, OR 97207. [2]Laboratory for Space Sciences, Washington University, St. Louis, MO 63130.

Introduction: As part of a continuing study of trace-element compositions of olivine in chondrules from UOCs such as Sahara-97210 (LL3.2) and Chainpur (LL3.4) [1], we have obtained the first trace element data for dusty olivine and coexisting clear olivine, in addition to normal igneous olivine, in chondrules from Chainpur. Dusty olivine contains micron-sized Ni-poor metal dust and is widely agreed to have formed by FeO-reduction of olivine during chondrule formation [2,3].

Dusty and clear olivines: We analyzed two porphyritic-pyroxene-olivine (PPO) chondrules that contain dusty-metal-bearing olivine and clear olivine. The clear olivine shows normal Fe-Mg zoning. The dusty and clear grains have the lowest concentration of Ni (10-22 and 16-34 µg/g, respectively) of all olivine analyzed to date, much lower than in normal igneous olivine from Chainpur (124 ± 35 µg/g, N = 13). Co contents are also low in both dusty and clear olivine (~6-12 and ~5 µg/g, respectively) compared to normal igneous olivine in Chainpur (25-130 µg/g). Low Ni and Co contents in dusty olivine were found despite analyzing metal dust with SIMS (~2 wt% overall in the dusty olivines, as inferred from EMPA data), indicating the olivine must be highly depleted in these elements. The P content of clear olivine (14-26 µg/g) is significantly lower than in coexisting dusty olivine (130-230 µg/g), and lower than in normal igneous grains (range 25-1000 µg/g, mean ~300 µg/g).

Formation of the PPO chondrules: Clear olivine probably formed by igneous crystallization from melts that were produced during the reheating event that caused metal dust to exsolve in dusty olivine. Similar, and low, abundances of Ni and Co in the dusty and clear olivine implies that they equilibrated with melt under reducing conditions sufficient to cause metal saturation and low $D^{ol/melt}$ values, corresponding to fO_2 values less than 3.9 log units below the CCO and NNO buffers [4]. This is consistent with the observed Fa contents of olivine (Fa_{4-9}) in the chondrules. Evidently, normal olivine crystallized with higher $D^{ol/melt}$ and fO_2 values, leading to higher Ni and Co contents. The low P content in clear olivine is also attributed to formation under low fO_2, but evidently P in the dusty olivine was out of equilibrium with the chondrule melt. Heating during chondrule formation must have been sufficiently long to allow Ni and Co to diffuse out of the dusty olivine, but not so long as to allow P to diffuse out. Based on Ni and Co diffusion data [5] and the size of the dusty relicts, this heating duration is estimated as about a few hours.

References: [1] Ruzicka A. and Floss C. (2004) *Lunar Planet Sci. XXV*, #1422. [2] Leroux H. et al. (2003) *Meteorit. Planet. Sci.* 38, 81-94. [3] Jones R.H. and Danielson L.R. (1997) *Meteorit. Planet. Sci.* 32, 753-760. [4] Ehlers K. et al. (1992) *Geochim. Cosmochim. Acta* 56, 3733-3743. [5] Morioka M. (1981) *Geochim. Cosmochim. Acta* 45, 1573-1580.

SEM-CL STUDY OF QUARTZ FROM Mt. OIKEYAMA-EVIDENCES ON A POSSIBLE IMPACT STRUCTURE IN JAPAN. M. Sakamoto[1], H. Nishido[2], A. Gucsik[3], K. Ninagawa[1], and T. Okumura[1], [1]Neba Elementary School, 80 Neba Village, Nagano, 395-0701 Japan [2]Okayama University of Science, Dept. of Applied Physics, Ridai-cho 1-1, Okayama, 700-0005, Japan, [3]University of West Hungary, Bajcsy-Zs. u. 4., Sopron, H-9400, Hungary. E-mail: ciklamensopron@yahoo.com

Introduction: The origin of the Mt. Oikeyama structure in Central Japan has been debated for many decades. The purpose of this study is to provide new information about scanning electron microscope-cathodoluminescence (SEM-CL) data of planar microdeformations in quartz samples to determine whether this area was formed by tectonic, regular geological processes or shock metamorphic events.

Experimental Procedure: SEM-CL imaging and CL spectral analyses were performed on selected polished thin sections coated with a 20-nm thin film of carbon in order to avoid charge build-up. SEM-CL images were collected using a scanning electron microscope (SEM), JEOL 5410LV, equipped with a CL detector, Oxford Mono CL2, which comprises an integral 1200 grooves/mm grating monochromator attached to reflecting light guide with a retractable paraboloidal mirror.

Results and Discussion: Gratz et al. [1] distinguished shocked quartz from tectonically deformed quartz by SEM on the HF-etched quartz, and reported differences between glass-filled Planar Deformation Features (PDFs-"pillaring" texture) and glass-free tectonic deformation arrays. These similarities of the shock-related pillaring texture and tectonic-related arrays in a quartz sample from Mt. Oikeyama are visible in the secondary image followed HF-etching. This indicates that the presence of glass-filled micro-cracks such as wide planar transformation lamellae might be related to the shock-metamorphic processes [1]. Seyedolali et al. [2] and Boggs et al. [3] revealed that planar microstructures in shocked quartz resulted from meteorite or cometary impact can be discriminated from other resemble features by SEM-CL image. Typical CL image of PDFs described by [3] is characterised by fine dark streaks with 1-2 μm thickness in bright luminescent background and sufficient parallelism of dark streaks with 5-20 μm spacing, where the texture of CL image is favourably compared with planar microstructures illustrated in petrographic optical image. Overwhelming parallel dark streaks observed in CL image of Oikeyama quartz are quite narrow in thickness of 1 to 2 μm or less near to effective resolution of CL imaging, whereas several broad dark bands with 5-10 μm thick can be recognised. The spacings of dark streaks are predominant in 3-5 μm. According to the verification by [3] parallel dark streaks in CL image of Oikeyama quartz could be unambiguously led to the evidence of PDFs. Consequently, all arguments of an impact origin of the Mt. Oikeyama and related rocks are based on interpretation of selected SEM-CL observations.

Acknowledgement: This work has been partly supported by the Hungarian Space Office (TP-293).

References: [1] Gratz A. J. et al. (1996) *Earth Planet. Sci. Lett., 142,* 513-521. [2] Seyedolali A. et al. (1997) *Geology 25,* 787-790. [3] Boggs S. et al. (2001) *Meteoritics Planet. Sci. 36,* 783-793.

CHICXULUB EJECTA PLUME FORMATION AND THE LINK WITH THE GLOBAL K-P BOUNDARY

T. Salge, L. Hecht and D. Stöffler. Museum of Natural History (Mineralogy), D-10099 Berlin, Germany. E-mail: tobias.salge@rz.hu-berlin.de.

Introduction: The Chicxulub target was composed of (1) a ~3 km thick sedimentary sequence, resulting in an extremely volatile-rich target, and (2) a crystalline silicate basement. A petrographic and chemical study of samples from the marine K-P site of El Guayal [1] ~520 km SE of Chicxulub and of selected samples from the UNAM-7 borehole near the crater rim [2] has been carried out.

El Guayal: An ~40 m thick carbonate megabreccia documents the failure of the Yucatán platform due to impact induced earthquakes [1]. The overlying ~10 m thick suevite-like sequence contains shocked minerals and altered (to clay minerals) silicate melt particles. Spherulitic carbonate melts are similar to rapidly quenched feathery calcite of the Y6 crater suevite [3]. Fusion of silicate melt with carbonate induced calcite recrystallisation at >750°C. CO_2 release is indicated by voids in silicate melt at the contact to the calcite. Accretionary lapilli <2 cm in size occur at the base of an upper 2.5 m thick subunit. They contain mainly <150 µm sized shocked and molten particles and were formed during a late stage of plume evolution in a turbulent steam condensing environment. Multiple laminations, each with decreasing grain size, document recurring heat increase [4]. In the clay unit on top of the suevite, a PGE-enriched impactor component was deposited together with shocked quartz and carbonate melt spheroids. This provides evidence linking the Chicxulub impact with the global K-P boundary. **UNAM-7:** Into the suevite of UNAM-7 307.85 m [2], altered (to clay) silicate melt particles were deposited in the liquid state as shown by reaction rims against matrix. Seawater interaction is indicated by Br, Cl and Sr enrichment of silicate melt particles. The underlying polymict sedimentary breccia of UNAM-7 381.40 m contains polygonal to interlobate calcite spheroids indicative for deposition in a molten state. The matrix is composed of microcrystalline calcite and microcrystalline to larger/euhedral anhydrite and shows a schlieren-like flow texture. Calcite degassing is indicated in anhydrite clasts by thin schlieren of microcrystalline calcite associated with voids. These observations suggest matrix formation by exothermic reaction of decomposed calcite (CaO) with water (slaking) and subsequent back-reaction with CO_2. Hence, anhydrite precipitated from sulphate-rich fluids heated >350°C by slaking and from silicate melt particles, analogous to processes related to VHMS deposits.

Conclusions: The following sequence of processes is suggested: (1) Vapour release by decomposition of water saturated sediments changed ejecta distribution from ballistic to flow-like transport. (2) Ejecta plume collapse separated suevite from impactor material that had been lifted into the stratosphere. (3) Fusion of the different target components initiated hot gas-driven lateral transport in a basal flow. (4) Accretionary lapilli formed in a coherent turbulent ash cloud.

Acknowledgements: This work is part of TS' PhD thesis. TS kindly thanks P. Claeys for providing samples, R. Tagle for PGE analyses and H. Stosnach for introduction to TXRF analyses.

References: [1] Grajales J. M. et al. 2000. *Geology* 28:307–310. [2] Urrutia-Fucugauchi J. et al. 1996. *Geofis. Int.* 35:125–133. [3] Claeys P. et al. 2003. *MAPS* 38:1299–1317. [4] Moore J. G. and Peck D. L. 1962. *J. Geol.* 70:182-193.

ON PLANETESIMAL MELTING AND CHRONOLOGY

I. S. Sanders, Dept. of Geology, Trinity College, Dublin, Ireland. E-mail: isanders@tcd.ie.

Basaltic meteorites, from their Al-Mg whole-rock model ages, were produced in a brief period between 3 and 4 million years (Myr) after CAIs [1,2]. Since two basaltic meteorites, Sahara 99555 and Asuka 1394, have precise Pb-Pb ages of 4566.2 and 4566.5 Ma respectively [1,3], the popular Pb-Pb age of 4567.2 Ma for CAIs [4] poses a conundrum. Also puzzling is the ^{182}W anomaly in iron meteorites, which suggests that metal cores formed < 1 Myr after CAIs [5].

Thermal modeling offers insights into the timing of melting. The model of [6] modified with initial ^{26}Al/^{27}Al, ^{60}Fe/^{56}Fe and decay energies used by [2] shows the dominant effect of accretion time on the melting of a planetesimal's insulated interior. If accretion happened within about 1 Myr of CAIs, heating would have outstripped melt percolation and led to wholesale meltdown and turbulent convection in all but the outer crust [6]. Sooner rather than later, a dense iron core would have separated, with its ^{182}W deficit. Little evidence of this early melting survives in meteorites other than irons, possibly because the molten silicate fraction was recycled by planetesimal disruption into chondrules [7]. Where accretion happened between about 1 and 1.5 Myr after CAIs it is likely that the rate of heating was slow enough to let basaltic partial melt segregate and reach the planetesimal surface between 3 and 4 Myr after CAIs, in agreement with the whole-rock Al-Mg ages. If accretion was 1.5 to 2 Myr after CAIs then heat loss would confine any melting to the planetesimal's deep interior, and accretion after 2 Myr would preclude melting. By then the unspent radioactivity would have fallen below the 1.6 kJ/g needed to melt dry primitive rock [7].

Basalt production is proposed here as a new anchor for the Al-Mg, Pb-Pb and Mn-Cr chronometers. In this case the two Pb-Pb ages of 4566 Ma [1,3] date eruption, making CAIs 4569.5 Ma, as shown by [1]. Also the eucrite whole-rock Mn-Cr isochron of [8] is taken to date eruption at 4566 Ma, making 'absolute' Mn-Cr ages based on the angrite anchor, LEW 86010, 1.5 Myr too young. This realignment of ages suggests that the 4567.2 Ma CAI age [4] was reset after CAI formation, and that the Pb-Pb and Mn-Cr systems in LEW 86010 may record different stages during cooling. However the basalt anchor improves I-Xe ages [9] (Shallowater becomes 4564.8 Ma due to the 1.5 Myr shift in Mn-Cr ages) and, pleasingly, the Hf-W age of CAIs shifts by 1.5 Myr to 4569.5 Ma [5].

Finally, could some iron cores predate CAIs as hinted at by [5]? One speculative option to explore is that CAIs themselves may have a planetary origin. Could they be condensates from a large early runaway that exploded catastrophically while heating and accreting? Could the vapour pressure in its superheated, totally molten centre have grown to exceed the pressure of its younger, thick and still cool overburden?

References: [1] Baker J. et al. 2005, *Nature* 436:1127-1131. [2] Bizzarro M. et al. 2005, *Astrophysical Journal* 632:L41-L44. [3] Amelin Y. et al. 2006, Abstract #1970. 37th Lunar & Planetary Science Conference. [4] Amelin Y. et al. 2002, *Science* 297:1678-1683. [5] Kleine T. et al. 2005, *Geochimica et Cosmochimica Acta* 69:5805-5818. [6] Hevey P.J. & Sanders I.S. 2006, *M&PS* 41:95-106. [7] Sanders I.S. & Taylor G.J. 2005, *Astronomical Society of the Pacific Conference Series* 341:915-932. [8] Lugmair G.W. & Shukolyukov A. 1998 *Geochimica et Cosmochimica Acta* 62:2863-2886. [9] Gilmour J.D. et al. 2006, *M&PS* 41:19-31.

THERMAL OUTGASSING OF ORDINARY CHONDRITIC MATERIAl – II. SENSITIVITY STUDIES.

L. Schaefer[1] and B. Fegley, Jr. [2] [1,2]Washington University, St. Louis. [1]laura_s@wustl.edu, [2]bfegley@wustl.edu.

Introduction: We modeled out-gassing of ordinary chondritic (OC) material. Results for our nominal model are described in our companion abstract [1]. In this abstract, we describe the sensitivity of our nominal results to (1) variations in P and T, (2) variable volatile (H, C, N, O, S) abundances, (3) kinetic inhibition of solid solutions, (4) solubility of C and N in metal, and (5) open (vs. closed) system behavior.

Methods: Our nominal model is described in [1]. In our sensitivity studies (1) – (4), we varied only one parameter at a time with all other parameters kept at their nominal values. Study (1): P varied from 1 – 5,000 bars at constant T, and T from 100 – 1600 K at constant P. Study (2): volatile abundances varied within the range observed in OCs. Study (3): equilibrium calculations were allowed to produce either pure phases or ideal solid solutions. Study (4): amounts of C and N dissolved in Fe metal were calculated. Study (5): an open system is modeled to first approximation as sequential equilibration of out-gassed volatiles within a layer, removal to a higher, cooler layer, and re-equilibration.

Results: (1) At low temperatures (T < 600 K), variation of pressure has little effect on major gas chemistry. At higher temperatures, the CH_4 abundance decreases with decreasing pressure, whereas H_2 increases. At high T (1200 K), CO > CH_4 for pressures less than 10 bars. While the major gas changes with pressure, oxygen fugacity is independent of total pressure.

(2) H was varied as both H and H_2O with no difference in effect. For large H abundances, the major gas is H_2, followed by CH_4 and H_2O. For very small H abundances, the total gas abundance drops (carbon forms graphite and/or carbides), and the major gas is N_2. Large C abundances do not change the overall gas chemistry, but at small C abundances, methane is only important for T < 500 K, with H_2 and H_2O more abundant at T > 500 K. Variable N abundances only affected N_2 and NH_3 abundances. Varying the S abundance had no affect on gas chemistry. There was no change in gas chemistry for O = 32 – 38 wt%. At lower O abundances, CH_4 and H_2 were the only abundant gases, and mineral assemblages were very reduced (e.g., CaS, MgS, Si_2N_2O).

(3) Calculation of solid phases as either pure phases or ideal solid solutions did not effect the equilibrium gas composition.

(4) N solubility in metal was neglected in the nominal runs. When allowed, solubility of nitrogen in Fe metal is only significant at higher temperatures, where ~ 9 % of total N_2 dissolves in γ-Fe. Even less N dissolves in Fe-Ni alloy. Roaldite (Fe_4N) did not form in any models. The amount of C dissolved in Fe metal is consistent with that observed in ordinary chondrites. When C solubility was not allowed ε-carbide (Fe_2C) formed instead.

(5) Outer layers of the parent body were highly enriched in volatiles in the open system calculations and hydrous phases such as mica, serpentine, talc formed. The equilibrium gas composition did not change significantly during open system out-gassing.

Acknowledgements: Supported by the NASA Astrobiology, Origins, and Outer Planets Research Programs. We thank K. Lodders for helpful discussions.

References: [1] Fegley, B., Jr. and Schaefer, L. 2006. this meeting.

COMPARISON OF HSE IN EARTH AND MOON

G. H. Schmidt[1]. [1]Institute of Nuclear Chemistry, University of Mainz, Germany. E-mail: gerhard.schmidt@uni-mainz.de.

The Moon can provide insight into the early development of the Earth, where the direct record of early evolution was destroyed by geological activity. Ages of polymict impactite samples show that the majority of the craters on the Moon's surface are at least 3.9 Ga old [1,2]. During solidification of the Earth's crust the surface was exposed to a similar flux of impacting asteroidal fragments as the Moon adding highly siderophile elements (HSE: Os, Ir, Ru, Pt, Rh, Pd) into the crust. The abundances of the HSE Ir, Ru, and Pd in the Earth's upper continental crust (UCC) derived on impact melt sheets and impactites are about 14 ± 8 pg/g Ir, 1.0 ± 0.6 ng/g Ru, and 2.0 ± 0.5 ng/g Pd. Elemental ratios of HSE, and Ni in the upper crust are highly fractionated in comparison to the Earth's mantle [3]. The abundance distribution indicates two groups of elements; (1) Os and Ir and (2) Ru, Pt, Rh, Pd, and Ni. The fractionation pattern from IIIAB iron meteorites and pallasites are comparable with a compilation of the present UCC data suggesting that the young UCC probably preserves an imprint of some of the major fractionation processes which have occurred in magmatic iron meteorites or pallasites.

The content of Ru in the UCC is in the same range as the indigeneous content of 2.01 ± 0.72 ng/g Ru derived from regression in Apollo 17 aphanitic impact melt rocks [4]. Palladium in the Earth's UCC is in the same range than the indigeneous content of 2.86 ± 0.94 ng/g Pd in poikilitic lunar melt rocks. It is assumed that HSE in these Apollo rocks were added from the impactor that formed the Serenitatis basin. The "indigeneous" HSE components in these rocks should have been added by >3.9 Ga impact event(s). Probably the nature of the materials that have bombarded the Moon (>3.9 Ga) was similar to the material that added these elements into the crust (magmatic iron meteorites and/or pallasites?).

In comparison to the Earth's mantle, Apollo 17 impact melt rocks show different noble metal patterns (see Fig.) than the "late accreted materials" on Earth (e.g. Ru/Ir in Earth's mantle is 2.01±0.12 [3], in lunar melt rocks, uncorrected for indigeneous Ru the Ru/Ir ratio is 1.68±0.09 [5]).

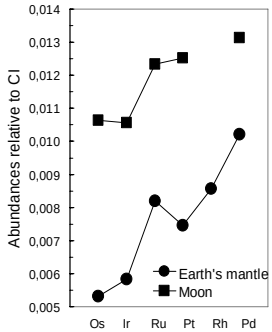

References: [1] Kirsten T. et. al. 1973. Proc. 4th Lunar Sci. Conf. 1757-1784. [2] Neukum G. et al. 1975. Proc. 6th Lunar Sci. Conf., *Geochim. Cosmochim. Acta.* 6:2597-2620. [3] Schmidt G. 2004. *Meteoritics & Planetary Science* 39:1995-2007. [4] Puchtel I.S. et al. 2006. Abstract #1428. 37th Lunar & Planetary Science Conference. [5] Puchtel I.S. et al. 2005. Abstract #1707. 36th Lunar & Planetary Science Conference.

THE DISRUPTION OF THE L CHONDRITE PARENT BODY AND THE GREAT ORDOVICIAN BIODIVERSIFICATION EVENT.

Birger Schmitz. Department of Geology, Lund University, SE-22362 Lund, Sweden. E-mail: birger.schmitz@geol.lu.se.

Evidence is growing in favor of that the disruption of the L chondrite parent body ca. 470 Ma led to a two orders of magnitude increase in the flux of extraterrestrial material to Earth during ca. 10-30 Myr [1-3]. Frequent impacts of large L chondritic asteroids during this period may have spurred one of the most important species diversification events in the history of life.

The most compelling evidence for an enhanced flux of extraterrestrial material is the high abundance of fossil meteorites (1-20 cm in diameter) in mid-Ordovician marine limestone in southern Sweden [1]. The meteorites are accompanied by abundant extraterrestrial chromite grains (>0.06 mm) dispersed throughout the limestone [2-3]. The stratigraphic distribution of the chromite can be reproduced in sections over 350 km distance in Sweden, and tentatively also in sections from central China. Petrographic studies of the fossil meteorites and the chemistry of meteorite-enclosed and sediment-dispersed chromite grains indicate an L chondritic origin. Cosmogenic isotopes in the chromite support an origin of the meteorites from an asteroid break-up event [4].

Considering that meteorites struck the Earth at an enhanced rate it is likely that the same applies for large asteroids. Support from this comes from an overrepresentation in the geological record of impact craters with a mid-Ordovician age [1]. For example, of 17 known craters on the Balto-scandian shield four have been dated with great confidence by chitinozoan stratigraphy to the middle or early late Ordovician. The recent discovery that the resurge deposits of the Lockne impact crater are extremely enriched in L chondritic chromite [5] shows that at least one of the four mid-Ordovician craters may be related to the disruption event. This is consistent with model simulations that indicate an enhanced flux of objects to Earth during 2-30 million years after major disruption events in the asteroid belt [6].

The so called Great Biodiversification Event during the mid to late Ordovician is one of the most important events in the history of life [7]. The biodiversity of invertebrates increased dramatically from a low in the Cambrian and early Ordovician to levels more similar to the present in the late Ordovician. Frequent bombardment of Earth by asteroids may have spurred these evolutionary changes. Repeated impacts created pressure on species to adapt to environmental perturbations. Previously, mid-Cenozoic faunal turnovers have been proposed to be related to a comet or asteroid shower [8], but although several craters of this age are known, there is no support from meteorite K-Ar gas retention ages for an asteroid shower of the same magnitude as in the mid-Ordovician. That impacts can have profound effects on life is obvious from the sequence of events at the Cretaceous-Paleogene boundary.

References: [1] Schmitz B. et al. 2001. *Earth & Planetary Science Letters* 194:1-15. [2] Schmitz B. et al. 2003. *Science* 300:961-964. [3] Schmitz B. and Häggström T. 2006. *Meteoritics & Planetary Science* 41:455-466. [4] Heck P. R. et al. 2004. *Nature* 430:323-325. [5] Alwmark C. and Schmitz B. 2006. *this volume.* [6] Zappala V. et al. 1998. *Icarus* 134:176-179. [7] Webby B. D. et al. (eds.) 2004. *The Great Ordovician Biodiversification Event*, 496 pp., Columbia University Press. [8] Tagle R. and Claeys P. 2004. *Science* 305:492.

THE PD-AG CHRONOMETER AND EARLY PLANETARY DIFFERENTIATION

M. Schönbächler[1,2], R. W. Carlson[1] and E. H. Hauri[1]. [1]Dept. of Terrestrial Magnetism, Carnegie Institution of Washington, 5241 Broad Branch Road, NW, Washington, DC 20015, USA [2]Dept. of Earth Sciences and Engineering Imperial College London, SW7 2AZ, UK E-mail: marias@imperial.ac.uk.

Introduction: The extinct ^{107}Pd-^{107}Ag isotope system can be used as a chronometer for the accretion and subsequent chemical differentiation of planetary bodies in a similar way as has been done with the ^{182}Hf-^{182}W system. In contrast to the refractory elements Hf and W, there is a distinct difference in volatility between more refractory Pd and moderately volatile Ag. This offers the potential not only to track metal-silicate differentiation processes but also volatility-related events.

Defining the initial ^{107}Pd abundance of the solar system is crucial for the application of the Pd-Ag system. Internal isochrons determined for iron meteorites yield initial ^{107}Pd/^{108}Pd ratios in the range of $1.5 - 2.5 \times 10^{-5}$ [1]. Whether these results reflect the initial abundance of ^{107}Pd in the solar system is unclear, because the absolute age corresponding to these internal isochrons is unknown. More recent studies suggest that the initial ^{107}Pd abundance might be up to an order of magnitude higher [2,3]. Further work is required to solve this issue.

A complication for the Pd-Ag chronometer is that Ag has only two isotopes, which makes it difficult to correct for chemically-induced mass-dependant fractionation. Mass fractionation effects in ε^{107}Ag are clearly displayed in ordinary chondrites, some of which show correlated Ag and Cd [4] isotopic variation. In contrast to ordinary chondrites, the CI, CM and oxidized CV chondrites possess the same Cd isotope composition as the Earth. In addition, carbonaceous chondrites show a considerable spread in Pd/Ag ratios (up to an factor 3) that could provide the opportunity to define a "whole rock" Pd-Ag isochron that represents a good estimate of both the initial ^{107}Pd abundance and ^{107}Ag/^{109}Ag of the solar system. By comparison with the Ag isotopic composition of the Earth, the Pd-Ag system has the potential to provide chronological constraints on the Earth's core formation.

Results: We have analyzed various chondrites including ordinary, enstatite and carbonaceous chondrites. Six different dissolution of Allende (CV3) yield an ε^{107}Ag of -0.6 ± 0.5 (2σ) relative to the NIST Ag standard. We will present additional data from CI, CM and oxidized CV chondrites whose analysis is in progress now. The comparison of Allende with the terrestrial Ag isotope composition determined from a variety of terrestrial basalts yields - depending on the model assumption - an age for an instantaneous Earth core formation of between 10 and 29 Myr after the start of the solar system. This is consistent with evidence from the Hf-W system.

References: [1] Chen J. H. and Wasserburg G. J. (1996), *in* Earth Processes: Reading the Isotopic Code, Geophysics Monograph '95, pp. 1-20. [2] Carlson R. W. and Hauri E. H. (2001) *Geochimica and Cosmochimica Acta*, 65: 1837-1848. [3] Woodland S. J. et al. (2005) *Geochimica and Cosmochimica Acta*, 69: 2153-2163. [4] Wombacher F. et al. (2003) *Geochimica and Cosmochimica Acta*, 67: 4639-4654.

A STONY METEORITE DISCOVERED BY THE MARS EXPLORATION ROVER OPPORTUNITY ON MERIDIANI PLANUM, MARS.

C. Schröder[1], R. Gellert[2], B.L. Jolliff[3], G. Klingelhöfer[1], T.J. McCoy[4], R.V. Morris[5], D.S. Rodionov[1], P.A. de Souza Jr.[6], A.S. Yen[7], J. Zipfel[8] and the Athena Science Team. [1]Inst. Anorg. und Analyt. Chemie, Johannes Gutenberg-Universität, Mainz, Germany. E-mail: schroedc@uni-mainz.de. [2]University of Guelph, Ontario, Canada. [3]Washington University in St. Louis, MO, USA. [4]Smithsonian Institution, Washington D.C., USA. [5]NASA JSC, Houston, TX, USA. [6]CVRD Group, Rio de Janeiro, Brazil. [7]JPL/Caltech, Pasadena, CA, USA. [8]Forschungsinstitut und Naturmuseum Senckenberg, Frankfurt/Main, Germany.

Introduction: The Mars Exploration Rover Opportunity is exploring the Meridiani Planum terrain of Mars. The area is characterized by a sulfate-rich bedrock largely covered by wind-blown basaltic sand and a hematite lag [1,2]. Only two large rocks (Bounce Rock and Heat Shield Rock) have been observed; they are interpreted as ejecta from a distant crater and an iron meteorite, respectively. Numerous cobbles (here, rock fragments > 1 cm), however, are scattered across the surface of Meridiani Planum [3]. Here we make the case for the possible meteoritic origin of one of these cobbles.

Results and Discussion: On sol 121 of its mission, Opportunity investigated a ~ 3 cm-sized cobble at the rim of Endurance crater. The cobble named FigTree_Barberton was analysed in situ by the Microscopic Imager (MI), the Alpha Particle X-ray Spectrometer (APXS), and the Mössbauer (MB) spectrometer. Barberton was too small to be brushed or abraded. Hence, the APXS spectra and, to a lesser degree, the MB spectra are contaminated by a thin dust covering. Owing to mission constraints, integration times for both spectrometers were limited. After subtraction of a dust component, APXS reveals a composition rich in Mg and Ni and poor in Al and Ca unlike any other material analysed by Opportunity. The Fe-bearing mineralogy revealed in MB spectra is dominated by the mineral olivine and contains metallic Fe in the form of kamacite. Nanophase ferric oxide may be attributed to dust contamination or alteration after deposition of the rock on the surface of Mars. The presence of kamacite suggests crystallization below the IW buffer. This makes a martian origin of Barberton unlikely, since SNC meteorites crystallized at or slightly below the QFM buffer and lack metallic Fe [e.g., 4]. Compared to a range of meteorites [5], Barberton is similar in Mg/Si, Ca/Si and Al/Si ratios to howardites and diogenites, but enriched in S/Si, Fe/Si and Ni and depleted in O. Mesosiderites provide a good match because they have a howardite-like silicate composition with additional metal and sulfide. Mesosiderites typically do not contain abundant olivine, although olivine diogenites are known. Imperfections in the dust correction may allow for other possibilities. In any case, it appears likely that Barberton is the first stony meteorite discovered on the surface of Mars.

References: [1] Squyres S.W. et al. 2004. *Science* 306:1698–1703. [2] Klingelhöfer G. et al. 2004. *Science* 306:1740-1745. [3] Jolliff B.L. et al. 2006. Abstract #2401. 37th Lunar & Planetary Science Conference. [4] Herd C.D.K. et al. 2001. *American Mineralogist* 86 :1015-1024. [5] Nittler L.R. et al. 2004. *Antarctic Meteorite Research* 17:231-251.

LARGE W-182 EXCESSES IN SILICATE INCLUSIONS OF IAB IRON METEORITES

Schulz T.[1,2,3], Muenker C.[2], Mezger K.[3] and Palme H.[1], [1] Institut für Geologie und Mineralogie, Universität zu Köln, Zülpicher Str. 49b, 50674 Köln, Germany, [2]Mineralogisch-Petrologisches Institut, Universität Bonn, Poppelsdorfer Schloss, 53115 Bonn, Germany, [3]Zentrallabor für Geochronologie, Institut für Mineralogie, Universität Münster, Corrensstr. 24, 48149 Münster, Germany.

The formation of non-magmatic iron meteorites during metal-silicate fractionation may have occured during condensation in the solar nebula [1] or in the interior of planets and planetesimals [e.g. 2-4]. Non-magmatic iron meteorites with silicate inclusions like the IAB-IIICD group are particularly interesting for the application of the Hf/W system as a chronometer for silicate-metal fractionation events during the early history of the solar system.

We have recently shown that silicate inclusions of four IAB iron meteorites display a very different W isotope composition than matrix and inclusion metals [6]. Both metals have ε_W values of around -3 and the corresponding silicates have excesses of about +6. One possibility to interpret the similar W-182 excesses but variable Hf/W ratios in the four silicate inclusions was to postulate a separate late stage thermal metamorphic event that re-equilibrated the silicate inclusions. This event must have taken place after Hf-182 was extinct. Further analyses of separated silicates were done to evaluate whether the uniform value of +6ε records a maximum W-182 excess or if there are still reservoirs with higher W-182 that were not equilibrated.

The measured matrix- and inclusion metals of the IAB meteorites Lueders, Landes and Campo del Cielo are indistinguishable from each other and range from -3.5 to -3 ε_w units. Newly prepared silicate separates of extremely high purity from the meteorite Campo del Cielo and Caddo County, however, yield highly radiogenic ε_w values of ca. +10 and ca. +30, respectively, similar to values obtained for eucrites. We suspect that these values represent Hf-182 decay in clinopyroxene, the major host phase of Hf in these inclusions.

Altogether the new results confirm that there is no complete equilibration between matrix metals and silicate inclusions in IAB iron meteorites. In some cases, the silicate inclusions may have internally equilibrated after Hf-182 was extinct, yielding less radiogenic ε_w. The inclusions that were not equilibrated preserved their highly radiogenic ε_w, thus providing time constraints on the parent body of the inclusions. Due to the very low exposure age of Caddo County (ca. 5 My) a cosmic ray effects can be neglected.

References: [1] Wasson, Proc. Intl. Geol. Cong. 24, 161-168 (1972); [2] Wasson et al., Z. Naturforsch. 35a, 781-795 (1980); [3] Choi et al., Geochim. Cosmochim. Acta 59, 593-612 (1995); [4] Kelly et al., Geochim. Cosmochim. Acta 41, 93-111 (1977); [5] Kleine et al., Geochim. Cosmochim. Acta 69, 5805-5818 (2005); [6] Schulz et al., LPSC XXXVII, #1401 (2006)

NEW DATA ON THE COOLING HISTORY OF THE H CHONDRITE PARENT BODY.

W. H. Schwarz[1], M. Trieloff[1], E. V. Korochantseva[1,2], A. I. Buikin[1,2]. [1]University of Heidelberg, Institute of Mineralogy, Im Neuenheimer Feld 236, D-69120 Heidelberg, Germany. E-mail: Winfried.Schwarz@min.uni-heidelberg.de, [2]Vernadsky Institute of Geochemistry, Kosygin St. 19, 119991 Moscow, Russia.

Introduction: In the early Solar System, ~4.6 Ga ago, the formation of asteroidal-sized solid bodies took place in less than 10 Ma, including the parent bodies of chondritic meteorites. Their early thermal histories have been constrained using various radiochronometer, in order to reconstruct heating mechanisms of thermal metamorphism, and structure and cooling history of their parent bodies (e.g. [1-6]).

^{40}Ar-^{39}Ar dating: 8 H chondrites with complete (U-Pb [5], Ar-Ar and ^{244}Pu fission track [6], MTCR [4]) chronologies indicate undisturbed cooling in a parent body heated by ^{26}Al. Here we present new ^{40}Ar-^{39}Ar data for different H chondrites to complement previously published ^{244}Pu fission track data [6]. Repeat analyses of Guarena (H6) yielded 4428±10 Ma, Mt. Browne (H6) 4486±5 Ma. Dhofar 323 (H5; host and xenolith) is 4510±7 Ma, the H4 chondrites Ankober, Beaver Creek, Quenggouk and Ochansk are between 4448±7 and 4526±6 Ma old (constants by [7]).

Discussion: Pu fission track cooling rates and densities in merrillite and orthopyroxene correlate with the Ar-Ar age of the meteorites (in principal higher for H4 chondrites and lower for H6 chondrites), as expected for cooling models of an onion shell layered body [1,2,5,6]. This conclusion holds for Guarena, Mt. Browne, Dhofar 323, Ochansk, and Beaver Creek. H6 Mt. Browne and H4 Beaver Creek were likely located close to the H6/H5 and H4/H5 boundaries. However, two H4 chondrites (Ankober and Quenggouk) have lower-than-expected absolute Pu FT densities and Ar-Ar ages, though both metallographic and Pu FT cooling rates are fast as for other H4 chondrites. We conclude that these meteorites were affected by an early impact on the parent body, thereby resetting the K-Ar clock and the Pu FTs, and subsequent fast cooling. Apparently, only part of the H4 material was affected and not redeposited into deep layers (in this case cooling would have been slow).

Conclusion: If the H chondrite parent body has been completely fragmented and reassembled affecting the interior H6 core [4] there should be meteorites with petrographic type H6, high metallographic and Pu cooling rates and at least very high (H4 like) Ar-Ar ages. This is not the case yet, and thus it is not necessary to postulate fragmentation and reassembling of the whole parent body. Instead, the “simple” cooling of a large asteroid (with several impacts on its surface affecting only part of the H4 layer) is a viable explanation for all data presented here and in the literature (e.g. [4-6]).

References:

[1] Herndon J.M. and Herndon M.A. 1977. *Meteoritics* 12:459-565. [2] Miyamoto M. et al. 1981. *Proc. Lunar Planet. Sci. Conf.* 12B:1145-1152. [3] Grimm R.E. 1985. *J. Geophys. Res.* 90(B2):2022-2028. [4] Taylor et al. 1987. *Icarus* 69:1-13. [5] Göpel C. et al. *EPSL* 121: 153-171. [6] Trieloff M. et al. 2003. *Nature* 422:502-506. [7] Steiger R.H. and Jäger E. 1977. *EPSL* 36:359-362.

NITROGEN AND NOBLE GASES IN ALHA 77005, A SMALL MARTIAN METEORITE FROM ANTARCTICA.

S. P. Schwenzer[1], S. Herrmann[1] and U. Ott[1]. [1]Max-Planck-Institut für Chemie, Joh.-J. Becherweg 27, D-55128 Mainz, Germany. E-mail: schwenze@mpch-mainz.mpg.de.

ALHA77005 is a small (482.5 g) Martian meteorite found in the 1977-1978 field season in Antarctica [1] and is – also in its noble gas patterns – most closely related to LEW88516 [2]. Its exposure age is ~3 Ma (mean of data given in [3, 4]), its terrestrial residence age (190 ±70) ka [3]. Besides its pristine petrography, alteration assemblages (observed by [5] and most likely of terrestrial origin) are noteworthy in the discussion of its noble gas inventory. To our knowledge, no nitrogen data have been reported so far, literature data on noble gases are: A complete set of He, Ne, and Ar data as well as concentrations of ^{84}Kr and ^{132}Xe are reported by [6, 7], Kr and Xe data by [8], and ^{36}Ar, ^{84}Kr and ^{132}Xe by [9]. He, Ne, Ar, and Kr data are given by [10], [11] focus on neon, [12] measured the whole set of 23 noble gas isotopes, and [13–15] performed Ar-Ar analyses.

Results: We measured nitrogen and noble gases on a pyroxene (26.7 mg) and an olivine (45.8 mg) separate, and report He and Ne data for a bulk sample (43.2 mg).

Helium. Comparable concentrations of ^{4}He were found in all three samples: $(33\pm3)*10^{-8}$ ccSTP/g (bulk), $(29\pm1)*10^{-8}$ ccSTP/g (olivine), and $(28\pm6)*10^{-8}$ ccSTP/g (pyroxene). The ratio ^{4}He/^{3}He is ~4.6, indicating presence of cosmogenic Helium only and complete loss of any radiogenic component.

Neon. As for ^{4}He, amounts of ^{22}Ne agree within error in all three samples: $(1.33\pm0.10)*10^{-8}$ ccSTP/g (bulk), $(1.19\pm0.01)*10^{-8}$ ccSTP/g (olivine), and $(1.16\pm0.01)*10^{-8}$ ccSTP/g (pyroxene). Our ^{21}Ne/^{22}Ne ratios fall into the range given in the literature, but are lower than predicted from theoretical calculations for GCR neon using the production rates as function of chemistry of [16]. Following [11] we consider contributions from SCR neon as the most likely explanation.

Nitrogen. Our preliminary data give 10.0±0.5 ppm of N_2 and 5.3±0.3 ppm in olivine and pyroxene, respectively.

Heavy noble gases. In the 1600° C step of our olivine separate we found the highest ^{129}Xe/^{132}Xe ratio measured in this meteorite so far: 1.87±0.05. It is accompanied by high (cosmogenic corrected) ^{40}Ar/^{36}Ar of 1790±76. While whole rock samples seem to be compromised by elementally fractionated air contamination (cf. also [12]), our results for the mineral separates agree well with the data found for pyroxenes and olivine by [9].

References: [1] McSween, H.Y. et al. 1979. *Science*, 204: 1201–1203. [2] Treiman A.H. et al. 1994. *Meteoritics*, 29: 581–592. [3] Schultz L., Freundel M. 1984. *Meteoritics*, 19: 310. [4] Meyer C. 2001. Mars Meteorite Compendium 2001; Houston. [5] Smith, J.V., Steele, J.M. 1984. *Meteoritics*, 19: 121–133. [6] Bogard D.D. et al. 1984. *GCA*, 48: 1723–1739. [7] Nagao K. 1987. *12th Symposium on Antarctic Meteorites*: 49–1; Tokyo. [8] Swindle T.D. et al. 1986. *GCA*, **50**: 1001–1015. [9] Bogard D.D., Garrison DH 1998. *GCA*, 62: 1829–1835. [10] Eugster O. et al. 2002. *MAPS*, 37: 1345–1360. [11] Garrison D.H. et al. 1995. *Meteoritics*, 30: 738–747. [12] Miura Y.N. et al. 1995. *GCA*, 59: 2105–2113. [13] Jessberger E.K. et al. 1981. *Meteoritics*, 16: 331–332. [14] Schaeffer O.A., Warasila R. 1981. *LPSC*, XII, 932–942. [15] Bogard D.D., Garrison D.H. 1999. *MAPS*, 34: 451–473. [16] Leya I. et al. 2000. *MAPS*, 35: 259–286.

METEORITICAL AND DYNAMICAL CONSTRAINTS ON FORMATION MECHANISMS FOR ASTEROIDS AND PLANETS.

Edward R. D. Scott. HIGP, University of Hawai'i at Manoa, Honolulu, Hawai'i 96822, USA. escott@hawaii.edu.

How, when and where did asteroids form? Recent advances in integrating radiometric ages from long and short-lived isotopes [1] and thermal modeling [2] provide a new framework for understanding planetesimal formation and suggest that the thermal histories of meteorite parent bodies are closely linked to their formation times and locations. Chondrule ages and properties show that chondrites accreted intermittently from diverse batches of chondrules and other materials over a 4 Myr period starting 1 Myr after CAI formation [3, 4]. Iron meteorites and achondrites come from bodies that accreted earlier, when ^{26}Al was more abundant [5, 6]. Two different accretion mechanisms have been offered to account for the long timescale of chondrule formation. 1) Chondrules accreted to the surface of pre-existing bodies, e.g., [7]. 2) Differentiated and chondritic parent bodies formed in separate locations at different times. The latter is more consistent with meteorite evidence and requires a revision in the starting conditions inferred for dynamical models of planet formation to allow planetesimal formation to last 5 Myr. Formation of differentiated and chondritic bodies in separate locations can be accommodated if most irons formed inside 2 AU, as Bottke et al. [8] proposed; rare C-rich differentiated meteorites like ureilites and IAB irons may have formed simultaneously beyond 3 AU. Chondrite parent bodies formed subsequently in the gap between these two locations. If planetary embryos formed in under 1 Myr at 1 AU, they would have excited nearby planetesimals and prevented late-forming bodies from accreting near early-formed bodies.

Formation of Jupiter: Dynamical models suggest that asteroids could not have accreted in the main belt if Jupiter formed before the asteroids, as some chondrule-formation models imply [7, 9]. Jupiter therefore reached its current mass >3-5 Myr after CAIs formed. This precludes formation of Jupiter via a gravitational instability <1 Myr after the solar nebula formed [9], and strongly favors core accretion models for the giant planets.

Other planetary systems: Extrasolar planets have unusual orbits compared to solar giant planets, which may reflect differences in formation times. Planets that form quickly could interact gravitationally with more massive disks and migrate faster and further. In addition, early-formed planets would be more susceptible to orbital perturbations caused by close approaches of sibling protostars, as these become less frequent over time.

References: [1] Kita N. T. et al. 2005. In *Chondrites and the Protoplanetary Disk*, Krot A. N., Scott E. R. D., and Reipurth B. (Eds.), Astronomical Society of the Pacific Conference Series 341:558-587. [2] Hevey P. J. and Sanders I. S. 2006. *Meteoritics and Planetary Science* 41:95-106. [3] Amelin Y. et al. 2002. *Science* 297:1678-1683. [4] Krot A. N. et al. 2005. *Nature* 436:989-992. [5] Kleine T. et al. 2005. *Geochimica et Cosmochimica Acta* 69:5805-5818. [6] Bizzarro M. et al. 2005. *Astrophysical Journal* 632:L41-L44. [7] Weidenschilling S. J. et al. 1998. *Science* 279:681-684. [8] Bottke W. F. et al. 2006. *Nature* 439:821-824. [9] Boss A. P. and Durisen R. H. 2005. *Astrophysical Journal* 621:L137-L140.

THE MAGMATISM ON MARS INFERRED FROM CHEMICAL COMPOSITIONS OF MARTIAN METEORITES.

N. Shirai and M. Ebihara. Department of Chemistry, Graduate School of Science, Tokyo Metropolitan University, Hachioji, Tokyo 192-0397, Japan E-mail: shirai@comp.metro-u.ac.jp

Introduction: Martian meteorites are divided into four major groups; shergottites, nakhlites, chassignites and ALH 84001. An idea that Martian meteorites were derived by remelting a common mantle source at different times is controversial [1]. To understand the linkage among Martian meteorites should provide us insights in considering the petrogenetic processes and magmatism on Mars. We conducted a chemical study of Martian meteorites to place constraints on the petrogenesis for Martian meteorites based on their chemical compositions.

Analytical procedures: We used three nuclear analytical methods (PGA, INAA and IPAA) and ICP-MS to determined major, minor and trace elements in Martian meteorites.

Result and Discussion: La/Th ratios are found to increase with decreasing La/Yb ratios among shergottites. However, nakhlites and chassignites are not on this observed trend. Given bulk partition coefficients for dominant minerals of the Martian mantle (olivine, pyroxene and garnet) [2], igneous processes involving such dominant minerals cannot produce the chemical characteristics for nakhlites and chassignites. Shirai and Ebihara [3] suggest that igneous processes involving apatite, epidote and/or zircon control the fractionation of La/Th and La/Yb for nakhlites and chassignites.

Using a multi-stage evolution model proposed by [4], we reported that majorite is responsible for chemical characteristics (Hf/Sm and La/Yb ratios) in Martian meteorites [5]. However, La/Th ratios for nakhlites cannot be produced by igneous process involving majorite. To overcome such a difficulty, we constructed the following petrogenetic processes based on a multi-stage evolution model. At the 1st stage, the majorite cumulate formed during the differentiation of Martian magma ocean at 4.553Ga, only 13Ma after the solar system formation. At the 2nd stage, the majorite cumulate was partially melted and the produced melt crystallized at 4.0Ga. At the nakhlites' crystallization age (1.26-1.37Ga), partial melting of the crystallized melt formed at 4.0Ga occurred. The produced melt and residue represent nakhlites and shergottites (QUE 94201, Y 980459, DaG 476, SaU 005 and Dho 019), respectively. Assuming that majorite was the only mineral present until 4.0Ga and that clinopyroxene and an accessory mineral (zircon, epidote and apatite) constituted the precursor material for Martian meteorites at the subsequent igneous process, we calculated chemical compositions of the melt and the solid (residue) produced at each stage. Our results suggest that zircon is responsible for the fractionation of La and Th in nakhlites. However a multi-stage evolution model doesn't explain chemical compositions of olivine-phyric shergottites. Thus, being different the inference from Nd isotopic compositions, chemical compositions of Martian meteorites support an idea of distinct multiple mantle sources.

References: [1] McSween H. Y. 2002. *Meteoritics & Planetary Science* 37:7-25. [2] Longhi et al. 1992. *Mars*, 184-208. [3] Shirai N. and Ebihara M. 2006. in press. [4] Shih. C.-Y. et al. 1999. *Meteoritics & Planetary Science* 34:647-655. [5] Shirai N. and Ebihara M. 2005. *Meteoritics & Planetary Science* 40:A140.

AIRBURSTS IN THE EARTH'S ATMOSPHERE: APPLICATION TO THE 1908 TUNGUSKA EVENT.

V.V. Shuvalov. Institute for Dynamics of Geospheres RAS, Leninsky pr. 38-1, 119334 Moscow, Russia. E-mail: shuvalov@idg.chph.ras.ru.

The Tunguska event [1] occured in 1908 was the largest aerial burst induced by asteroidal (or cometary) impact and recorded in human history. The term aerial burst defines a variety of impacts which do not produce craters, but produce strong atmospheric (radiation, shock waves, acoustic-gravity waves) and possibly surface (devastations and fires) effects. There are good reasons to believe that Tunguska-like and much larger aerial bursts continiously occured during geological history.

Three types of airbursts can be considered: surface impact (when a hot jet or fireball touches the ground), Tunguska-like phenomena (when a jet or fireball do not reach the ground but produce fires and devastation), and meteor-like phenomena (when there is a bright flash but no surface effects). The purpose of this work is to study numerically the influence of impact angle and projectile properties (velocity and density) on the processes accompanning aerial burst.

I modeled the impacts of spherical stony and cometary projectiles of different sizes (from 20 to 1000 m) at velocities U=50 and 20 km/s. Impact angles were 90, 45, 30, 15, and 5 degree (to horizon).

To perform numerical simulations I used the model developed by Shuvalov and Artemieva [2]. For all trajectory angles α I solved numerically a 2D problem with effective atmospheric scale height $H/\cos(\alpha)$, where H is the normal atmospheric scale height. Initial altitude (at t=0) was 70 km.

Numerical simulations show that in all the cases under consideration the projectile begins to deform under increasing aerodynamic loading forming a typical pan cake-like structure, then it transforms into a debris jet consisting of meteoroid vapor, fragments, and shock compressed air. After total evaporation of projectile debris a gaseous jet consisting of vapor and hot air is formed. An important feature is that the disruption and total evaporation of a projectile occurs at a high velocity which is close to the pre-entry velocity. This scenario is typical for both cometary and stony meteoroids.

The impact velocity very slightly influences the altitude of projectile disruption and deceleration. The influence of projectile density is much stronger. A 100-m-diameter cometary projectile with a density of 0.9 g/cm^3 produces approximately the same effect as a 100-m-diameter stony projectile with a density of 3.5 g/cm^3. The impact angle is also an important parameter. Solid fragments of cometary meteoroids with initial diameter exceeding 70 m reach the ground in a vertical impact whereas a 1000-m-diameter comet burns totally in the atmosphere in a very oblique 5 degree impact.

Numerical simulations show that 30 to 45 degree oblique impacts of both a 60-m-diameter stony meteoroid and a 100-m-diameter cometary meteoroid produce effects similar to those observed in the 1908 Tunguska event.

Acknowledgement: This publication is based on work supported by Award No. RUG-2655-MO-05 of the U.S. Civilian Research and Development Foundation.

References: [1] Vasilyev N. A. 1998. *Planetary and Space Science* 46(2/3):129 - 150. [2] Shuvalov V. V. and Artemieva N. A. 2002. *Planetary and Space Science* 50/2:181-192.

STATISTICAL ASSESSMENT OF MAJOR ELEMENT COMPOSITION OF MOLDAVITES FROM THE CHEB BASIN.

R. Skála. Institute of Geology, Academy of Sciences of the Czech Republic, Rozvojová 269, CZ-16500 Praha 6, Czech Republic. E-mail: skala@gli.cas.cz.

Introduction: The Tertiary and Quaternary sediments of the Cheb Basin are known as one of the sites where Central European tektites are found in a considerable amount. Up to now, between 1200 and 1500 individual pieces were found there. This constitutes the third most prominent source of moldavites known. The areas in and around the Cheb Basin can be considered a separate sub-field. This sub-field is the closest one to the source crater of moldavites – the Ries impact structure.

Samples and Data Processing: For the current study, totally 24 moldavites from the Cheb Basin, were selected. As a reference, a set of 12 moldavites from three different South-Bohemian localities and 3 Moravian moldavites were chosen. All these samples were prepared as polished (thin) sections and analyzed with an electron microprobe for major elements. Later multivariate statistical tests allowed to exclude outliers. The data with outliers left out were subsequently processed with the statistical packages SYSTAT (version 11).

Factor Analysis was carried out separately for the data collected for the samples from the Cheb Basin and those for South Bohemian and Moravian moldavites. Both groups of moldavites, applying the Keiser criterion, produce two-dimensional factor loading plots with three distinct clusters. These three components accounted for 84 % of the total variance in the case of Cheb moldavites and for 82 % in the case South Bohemian and Moravian samples. Individual clusters for the samples from the Cheb Basin consist of: (1) SiO_2, (2) TiO_2, Al_2O_3, FeO, and Na_2O, and (3) CaO, MgO, and K_2O. For other group of samples, however, the results differ: factor loadings are somewhat rotated and, more importantly, K_2O groups with cluster (2) instead of (3); which is identical to the data given in [1].

Cluster Analysis provided a few relatively well defined and separated groups. The largest distance from remainder of the data was recorded for three samples (Chlum, Jankov, and Štěpánovice). Other samples are well clustered with very small mutual distances – one of the clusters contains almost exclusively the samples from the Cheb Basin whereas the remaining samples are mixed in other cluster.

Conclusions: Factor analysis showed striking difference between the chemical composition of Cheb moldavites and moldavites from remaining part of the moldavite strewn field on the Czech Republic territory. It possibly reflects different composition of the source material. Simultaneously, cluster analysis revealed that some of the Cheb moldavites are chemically close to those from South Bohemia.

Acknowledgements. This work was funded by the grant of the Czech Science Foundation (GAČR) No. 205/05/2593 and falls within the research plan AV0 Z30130516 of the Institute of Geology AS CR.

References: [1] Delano J.W. et al. (1988) *2nd Int. Conf. Natur. Glasses*. Charles University, Prague, pp. 221-230.

'THE CURATOR'S DILEMMA' REVISTED – CHALLENGES FOR METEORITE COLLECTIONS IN THE 21st CENTURY

C. L. Smith[1] and L.C. Welzenbach[2]. [1]Department of Mineralogy, The Natural History Museum, Cromwell Road, London, SW7 5BD, UK. C.L.Smith@nhm.ac.uk. [2]Department of Mineral Sciences, National Museum of Natural History, Smithsonian Institution, Washington, DC 20560-0119

Introduction: The original article 'The Curator's Dilemma' was first published in Meteoritics nearly 30 years ago [1]. With the advent of new investigative techniques, new avenues of research, and important new curatorial methods it is timely to restate the challenges faced by meteorite curators. M. H. Hey [1] described the greatest challenge of collection curation as '*two diametrically opposed duties: On the one hand, he [the curator] must make material available for research and study, and on the other, he must preserve the material in his care for enjoyment and study by future generations*.' Hey goes on to outline seven criteria in order to strike a balance, all of which are still appropriate and applicable today.

The Challenges: *The cost of doing business*. For more than 100 years, our collections have been providing meteorites to the scientific community. Evolving technology, new areas of research and the sheer number of scientific investigations place significant demands on dwindling or even non-existent museum resources, especially for collections that are very small relative to most museum populations. Those same new research fields may impact storage practice and accessibility. For example, samples stored in a Teflon bag may affect C isotope studies in astrobiological investigations. More research is needed to identify the effects of storage practices on the meteorites. Ideally we would apply clean room models for storage and handling, but must consider accessibility as well as cost. A solution may be to use limited clean room storage for samples where terrestrial contamination is the most detrimental to scientific studies e.g. SNCs, carbonaceous chondrites.

Acquisition of new meteorites has also evolved from a century ago. We now compete against a large population of collectors for smaller amounts at greater expense. More meteorites on the market enables us to broaden the range of meteorite types in our collections, but smaller quantities require a more detailed approach to sample allocation. First we direct the investigator to institutions with main masses. We use our broad understanding of the different investigative methods and techniques used to ensure that allocation of rare and limited material is resolving a fundamental problem. Although modern techniques allow for detailed information (e.g. about single isotopes or unique compounds) to be gathered from small fragments of material, the curator would like to see coordinated studies, allowing for as much information to be gathered from the material as possible.

Information management has become one of the foremost tools used for accountability, strategic planning and collections management. The NHM and NMNH manage the meteorite inventory and publication information with the 'EMU' database system. The power and flexibility of EMU allows us to develop new policies and procedures that help us address our diametrically opposed duties as well as streamlining requirements of accountability and providing us with quick reference to information for the increasing number of diverse and complex requests.

References: [1] Hey M. H. 1969. *Meteoritics*, 4:253-255.

SIMULTANEOUS ACCRETION OF DIFFERENTIATED OR METAMORPHOSED ASTEROIDAL CLASTS AND CHONDRULES.

A. K. Sokol and A. Bischoff. Institut für Planetologie, Wilhelm-Klemm-Str. 10, 48149 Münster, Germany. E-mail: sokola@uni-muenster.de.

The idea that certain meteorites represent samples of "second-generation" parent bodies (daughter asteroids) formed after collisional destruction of "grandparent" planetary bodies has been discussed earlier (e.g., [1-3]). Recent high-precision Hf-W and Al-Mg isotopic studies on differentiated meteorites indicate that differentiation on planetesimals occurred early, within ~3 Ma of the start of the solar system (e.g., [4-6]). Thus, accretion of differentiated planetesimals pre-dated that of undifferentiated planetesimals. Chondrites derive from relatively late formed planetesimals that may have formed by re-accretion of debris produced during collision disruption of first-generation planetesimals.

Increasing evidence is found for accretion of metamorphosed or differentiated planetesimal clasts with chondrules at a time, when chondrite parent bodies formed. In the case differentiated and metamorphosed "precursor" asteroid were destroyed prior to chondrites parent body formation, fragments of these earlier bodies may have been mixed with later formed chondrules and should exist in Type 3 or other primitive chondrites.

In some of the most primitive chondrites (Krymka, Adrar 003, Acfer 094)), we have found unusual fragments, which seem to have suffered thermal metamorphism. They look like typical type 6 lithologies, having 120° grain boundary junctions. In contrast to their host rocks all these inclusions show a homogeneous composition of minerals. They are chemically equilibrated. Most of them also contain coarse-grained plagioclases.

Some other observed clasts have igneous textures. Granitoidal and andesitic fragments in the ordinary chondrites Adzhi-Bogdo and Study Butte [7,8] indicate mixing of achondritic fragments and chondritic components. Also, the dark inclusions in CR and CH chondrites may be excellent witnesses to document formation of the final parent body by secondary accretion [3,9].

The existence of phases with high Al/Mg ratios in the observed inclusions offers a possibility for dating the time difference between the formation of these clasts and chondrules or CAIs using the Al-Mg chronometer. This work is in progress.

References: [1] Hutchison, R. 1996. In "*Chondrules and the Protoplanetary Disk"* (eds. R.H. Hewins, R.H. Jones, E.R.D. Scott), 311-318, Cambridge Univ. Press. [2] Bischoff A. 1988. *Meteoritics & Planetary Science* 33:1113-1122. [3] Bischoff A. and Schultz L. 2004. *Meteoritics & Planetary Science* 39: A15. [4] Bizzarro M. et al. 2005. *Astrophys. J.* 632:L41-L44. [5] Baker et al. 2005. *Nature*: 436, 1127-1131. [6] Kleine T. 2005. *Geochim. Cosmochim. Acta* 69:5805-5818. [7] Bischoff A. et al. 1993. *Meteoritics* 28:570-578. [8] Fredriksson K. et al. 1989. *Z. Naturforsch.* 44a:945-962. [9] Bischoff A. et al. 2006. In "*Meteorites and the Early Solar System II"* (eds. D. S. Lauretta and H. Y. McSween Jr) 679-712, University of Arizona, Tucson.

PERCOLATION OF Fe-FeS MELTS THROUGH AN OLIVINE MATRIX. A STUDY WITH A CENTRIFUGING PISTON CYLINDER

G. Solferino[1], N. Bagdassarov[2] and M. W. Schmidt[1]. [1]Institute for Mineralogy and Petrology, ETH Zurich. E-mail: solferino@erdw.ethz.ch. [2]Institut fuer Geowissenshaften, J. W. Goethe Universitaet.

Theories about the formation of the Earth's core postulate the segregation of molten iron-sulfide material through solid silicates [1]. The efficiency of this mechanism has not yet been proved and is still under discussion. The present study aims to establish the percolation threshold [2] for a simplified composition representative of the Earth's core and silicate mantle and to verify whether and under which conditions buoyancy driven segregation of such melts is a feasible process. Starting materials are iron-sulfide powder (on the eutectic composition of the Fe-FeS system) mixed with natural (S. Carlos) olivine powder. Experiments were performed in a standard end-loaded piston cylinder and in the newly developed centrifuging piston cylinder. With the centrifuging piston cylinder it is possible to spin a small press (standard 14 mm diameter, salt-pyrex assembly) to a maximum speed of 2900 rpm (equivalent to an acceleration of 3000g) at experimental conditions to 1.5 GPa and 1300°C.

A series of static and centrifuge experiments were performed using iron-sulfide plus olivine mixtures in double Pt-Graphite capsules (highly reducing conditions). No oxygen was detected in the melt pools (EDS measurements performed with an EMPA, Jeol JXA-8200) after the experiments. BSE images of quenched samples show interconnection of the melt in samples with 20 vol. % of iron-sulfide, whereas at 10 vol. % the melt is located in isolated pockets and in triple junctions. Centrifuge experiments were performed with mixtures containing 20 vol. % of melt in an olivine matrix and an additional thin layer of pure iron-sulfide on top of the olivine-melt. No sign of a melt displacement towards the bottom of the capsule was observed, although theory predicts melt segregation velocities of about 40 mm/h at 100g [3]. A reason for this behavior could be a high surface tension of the metallic-anionic melt that hinders its mobility in the inter-grain space. In a different series of centrifuge experiments, on olivine plus silicate melt, we have shown, that melt segregates (towards the top of the capsule), proving that the experimental set-up is proper to study percolation in partially molten systems. Thus, the absence of segregation for the iron-sulfide melt cannot be ascribed to an experimental flaw.

In conclusion, percolation of metallic-rich melts through a solid silicate matrix does not seem a plausible mechanism for core formation in terrestrial planets (at least in absence of shear deformation) at reducing conditions.

References: [1] Ringwood A. E. 1990. In *Origin of the Earth and Moon*: 101-134. [2] von Bargen N. and Waff H. S. 1986. *Journal of Geophysical Research* 91: 9261-9276. [3] McKenzie D. 1989. *Earth and Planetary Science Letters* 95: 53-72.

THE GLUE THAT BINDS: CONSOLIDATION PROCESSES FOR PLANETARY MATERIALS

J.G. Spray, Planetary and Space Science Centre, Department of Geology, University of New Brunswick, 2 Bailey Drive, Fredericton, New Brunswick, E3B 5A3, Canada (jgs@unb.ca)

Introduction: On Earth, the transformation of unconsolidated sediment (e.g., sand) to rock (sandstone) occurs via the process of lithification. Lithification typically occurs via burial within the upper crust at <150 EC, at depths <5 km in the presence of liquid H_2O. Liquid H_2O is critical to the process of lithification because it is the transporting medium for dissolved and suspended ions and mineral species, which eventually precipitate as a cement that binds the unconsolidated grains. Lithification also applies to sedimentary deposits formed by precipitation of minerals from aqueous solutions at surface, or near-surface, conditions (e.g., to generate sulfate or carbonate-rich evaporite rocks). However, for many planetary bodies in our solar system, there are no large sources of liquid H_2O to facilitate the lithification process. Despite the absence of water on such bodies, the development of consolidated fragmental material is commonplace. This material, typically in the form of breccias, is a relatively coherent rock, yet the nature of the "glue" that binds the fragments is not well understood. Clearly, other processes are responsible for the lithification that we take for granted in the sedimentary rocks developed on our wet planet. This work explores these processes.

Ices and Melts: For certain planetary bodies, unconsolidated material may be bound by ices, such that it possesses rock-like properties in terms in strength and behaviour. In the absence of H_2O, unconsolidated semi-molten material can be lithified by welding and compaction (e.g., certain pyroclastic discharges that fall and accumulate to form ignimbrites). This requires the production of hot volcanogenic or impact ejecta.

Consolidation Processes: In this work we explore the nature of the binding medium in different types of lunar breccia collected during the Apollo15, 16 and 17 missions, in meteorites of the howardite, eucrite and diogenite (HED) class and in laboratory shocked lunar regolith samples [1,2]. Analytical scanning electron microscopy (SEM) and field emission SEM are used to explore the microstructures. The samples are grouped as: (1) being primarily derived from unconsolidated lunar regolith; (2) impact melt rocks, and (3) samples that were primarily derived from solid rock that were impact brecciated. There is a significant overlap between these groups. Features that affect the cohesiveness and coherence of the rock are given particular attention. For this study, *bridges* are necks between grains, *intergranular melts* are melts that have between grains, *fused grains* are grains that are joined at a contact interfaces with no visible neck, and *annealed fractures* are fractures that have been partially or totally closed by either diffusion across the fracture or melting either side of the fracture. The various mechanisms of lithification are explored and discussed. Localized shock heating appears to be the dominant welding process.

References: [1] Schaal, R. B. et al. (1979) *Proc. Lunar Sci. Conf. 10th*, 2547-2571.
[2] Schaal, R. B. and Hörz, F. (1980) *Proc. Lunar Sci. Conf. 11th*, 1679-1695.

ANALOGOUS EXPERIMENTS ON CHONDRULE FORMATION USING RAPID IR-LASER HEATING

T. Springborn[1], T. Poppe[1], C. Güttler[1], J. Blum[1], and J. Wasson[2], [1]Institute für Geophysik und extraterrestrische Physik, Technische Universität Braunschweig, Mendelssohnstr. 3, 38106 Braunschweig, Germany, t.springborn@tu-bs.de. [2]Institute for Geophysics and Planetary Physics, University of California, 405 Hilgrad Avenue, Los Angeles, CA 90095-1567 USA

Introduction: Chondrules witness an energetic process which a large fraction of solar system material underwent in the time of planet formation. The chondrule precursors were porous dust aggregates composed of micrometer-sized major silicate and minor grains together with recycled chondrules. Chondrules formed by rapid melting by an unknown process in free space followed by rapid cooling. To investigate the formation conditions of first-generation chondrules, we have started an experimental study aiming at the transformation of porous dust samples to melt spherules via IR-laser irradiation. We use dust samples of micrometer-sized grains of iron, SiO_2, obsidian, albite, fayalite, and peridot, and mixtures thereof. The samples which have a typical mass of 2 mg, are irradiated for up to 10 seconds by a 30 W IR laser at ambient air pressures between 1 bar and 10^{-5} mbar. In some experiments the samples cooled in free fall.

First Results: A few samples (SiO_2) were not transformed because too little radiation was absorbed and some samples exploded. In most samples, 10–80% of the initial material was thermally processed. In about 50 experiments, spherules of chondrule size were formed, after some experiments even several spherules were found. We embedded some samples in epoxy resin and sectioned them, prior to microscopy. The samples analyzed so far are often porous, some contain large bubbles, and mostly, melting had not been complete but occurred to a varying extent. Assuming that roughly 2 kJ/g are required for melting [1], a first estimate of the energetic efficiency (energy consumed for melting/heating energy) is in the order of 1%.

Conclusion: For the first time, we produced chondrule-sized melt spherules from aggregates of micrometer-sized dust grains by electromagnetic radiation heating under conditions relevant for the formation of first-generation chondrules. However, unlike chondrules, most spherules produced up to now are porous or contain large bubbles. The experimental study is still in progress, and a final assessment will only be possible after further experiments.

Reference: [1] Wasson, J.T., 1996, Chondrule formation: Energetics and length scales, In: *Chondrules and the Protoplanetary Disk*, R.H. Hewins, R.H. Jones, E.R.D. Scott (eds.), Cambridge University Press, 45-54

THE DISTRIBUTION OF INCLUSIONS IN A SINGLE LARGE PRESOLAR SILICON CARBIDE GRAIN.

F. J. Stadermann[1] , T. Stephan[2], A. S. Lea[3] and C. Floss[1]. [1]Laboratory for Space Sciences, Washington University, St. Louis, MO 63130, USA. E-mail: fjs@wustl.edu. [2]Institut für Planetologie, Universität Münster, 48149 Münster, Germany [3]Pacific Northwest National Laboratory, Richland, WA 99352, USA.

The Murchison LS+LU presolar grain separation fraction contains large SiC grains with sizes above 2 µm [1]. A previous study of this SiC size fraction found two morphological types: irregular to round grains and blocky grains with flat surfaces [2]. We have performed detailed elemental and isotopic characterizations of a single 15 µm x 20 µm SiC grain of the latter type. We used complementary imaging techniques of SEM, NanoSIMS, ToF-SIMS, and Auger spectroscopy to determine the types and distributions of various inclusions in this unusually large SiC grain.

An initial NanoSIMS bulk C and N isotopic measurement of this particle identifies it as a likely mainstream type of SiC grain [e.g., 3] with $^{12}C/^{13}C = 54.1 \pm 0.1$ and $^{14}N/^{15}N = 447 \pm 26$. Subsequent O imaging yielded a low secondary ion signal, but indicated a heterogeneous distribution of numerous sub-micrometer spots with elevated O signals. These spots were clearly correlated with minute inclusions that were brought to the surface and then rapidly consumed by the primary ion beam sputtering. The O isotopic compositions of all spots, as well as the integrated composition of the remainder of the SiC are normal within errors. This indicates that the measured O may not be indigenous to the particle and that the O yield in the vicinity of inclusions may be artificially enhanced, similar to what has been observed in studies of internal grains within presolar graphites [4].

In an effort to determine the nature of the inclusions, we examined the particle with ToF-SIMS, in both positive and negative secondary ion modes, and with scanning Auger spectrometry. The latter technique for high spatial resolution elemental imaging is an ideal complement to NanoSIMS isotopic imaging measurements, because the volume of material analyzed by both techniques is virtually identical [5-7].

Imaging of the surface of the SiC grain showed Ti-V hotspots, which are likely to be TiC inclusions, as has been observed elsewhere [8]. We also observed hotspots of Al and of (not spatially correlated) Ca. Some of the inclusions appear to be correlated with steps or boundaries within the SiC grain structure. We will continue with another round of NanoSIMS measurements to determine the isotopic composition of the inclusions.

References: [1] Amari S. et al. 1994. *Geochimica et Cosmochimica Acta* 58, 459-470. [2] Virag A. et al. 1992. *Geochimica et Cosmochimica Acta* 56, 1715-1733. [3] Meyer B. S. and Zinner E. 2006. in *Meteorites and the Early Solar System II*, Lauretta D. and McSween Jr. H. Y. (eds.) U. of Arizona Press. [4] Stadermann F. J. et al. 2005. *Geochimica et Cosmochimica Acta* 69, 177-188. [5] Stadermann F. J. et al. 2005. *Meteoritics & Planetary Science* 40: 146. [6] Stadermann F. J. et al. 2006. Abstract #1663. 27th Lunar & Planetary Science Conference. [7] Floss C. et al. 2006. *Geochimica et Cosmochimica Acta* 70, 2371-2339. [8] Stroud R. M. and Bernatowicz T. J. 2005. Abstract #2010. 26th Lunar & Planetary Science Conference.

Acknowledgements: Some of the Auger measurements were performed with the PHI 700 demonstration instrument at Physical Electronics in Chanhassen, Minnesota.

MINERALOGY AND PETROLOGY OF COMET WILD2 NUCLEUS SAMPLES — FINAL RESULTS OF THE PRELIMINARY EXAMINATION TEAM.

Stardust Mineralogy/Petrology Subteam**:** Michael Zolensky[1], Phil Bland[2], John Bradley[3], Adrian Brearley[4], Sean Brennan[5], John Bridges[6], Donald Brownlee[7], Anna Butterworth[8], Zurong Dai[3], Denton Ebel[9], Matt Genge[2], Matthieu Gounelle[10], Giles Graham[3], Jeff Grossman[28], Lawrence Grossman[11], Ralph Harvey[12], Hope Ishii[3], Anton Kearsley[13], Lindsay Keller[1], Alexander Krot[14], Falko Langenhorst[27], Antonio Lanzirotti[15], Hugues Leroux[16], Graciela Matrajt[7], Keiko Messenger[1], Takashi Mikouchi[17], Tomoki Nakamura[18], Kazumasa Ohsumi[19], Kyoko Okudaira[20], Murielle Perronnet[1], Frans Rietmeijer[4], Steven Simon[11], Thomas Stephan[21], Rhonda Stroud[22], Mitra Taheri[22], Kazu Tomeoka[23], Alice Toppani[3], Peter Tsou[24], Akira Tsuchiyama[25], Michael Velbel[29], Iris Weber[21], Mike Weisberg[26], Andrew Westphal[8], Hajime Yano[20], Thomas Zega[22]. [1]NASA JSC (email: michael.e.zolensky@nasa.gov), [2]Imperial College, [3]Lawrence Livermore National Lab., [4]Univ. New Mexico, [5]SLAC, [6]Open Univ., [7]Univ. Washington, [8]Univ. California, Berkeley, [9]American Museum of Natural History, [10]Muséum National D'Histoire Naturelle, [11]Univ. Chicago, [12]Case Western Reserve Univ., [13]Natural History Museum, [14]Univ. Hawaii, [15]Brookhaven National Lab, [16]Univ. Sciences et Technologies de Lille, [17]Univ. Tokyo, [18]Kyushu Univ., [19]Inst. Materials Structure Science-KEK, [20]JAXA-ISAS, [21]Univ. Münster, [22]Naval Research Lab., [23]Kobe University, [24]JPL, [25]Osaka Univ., [26]Kingsborough Community College, [27]Inst. für Geowissenschaften, [28]US Geol. Survey, [29]Michigan State Univ.

Introduction: The sample return capsule of the Stardust spacecraft was successfully recovered in northern Utah on January 15, 2006, and its cargo of coma grains from Comet Wild 2 has now been the subject of intense investigation. This presentation will present the "final" results from the mineralogical and petrological analyses that will have been performed.

Mineralogy/Petrology: Although one month does not appear to be much time, it has been sufficient to permit numerous analyses (E-beam, Synchrotron XRD, spectroscopy, etc) to have been performed to permit some understanding of the following fundamental sample issues:

(1) Comet nucleus mineralogy and petrology, and grain physical properties

(2) Sample variability

(3) Type and degree of sample alteration by the collection process, and subsequent sample handling

(4) Sample documentation and handling procedures

(5) Comparisons to what was reported by the Deep Impact Mission to Comet Temple 1

Future of the Samples: Following the close of sample preliminary examination, Stardust samples will be made available to the larger community as are lunar samples, IDPs, and Antarctic meteorites. A sample "catalog" will be available at the JSC Curation website (http://curator.jsc.nasa.gov/stardust/index.cfm). A dedicated peer review committee will consider all sample requests. The Stardust interstellar tray is being scanned in the Cosmic Dust Lab; when this operation is complete (~Christmas 2006) the Cosmic Dust Lab will be reopened for business.

TIME DEPENDANT ENRICHMENT OF URANIUM IN OMAN DESERT CHONDRITES.

Ch. Stenger[1], U. Krähenbühl[1] and B.A. Hofmann[2]. [1]Department of Chemistry and Biochemistry, University of Bern, Freiestr. 3, 3012 Bern, Switzerland. E-mail: ch_stenger@students.unibe.ch,[2]Natural History Museum Bern, Bernastr. 1, 3005 Bern, Switzerland

Introduction: Surfaces of chondritic meteorites collected in the deserts of Oman in 2001-2003 are exposed to the often much higher concentrations of elements of interest in the desert soils. In the case of Uranium the abundance levels for the soils are about 500 times higher than the one measured for chondrites. The enrichment of this element found on the surface on meteorites and its diffusion into the interior are investigated.

Experiments:. Three H chondrite finds of similar size were studied for their Uranium concentrations showing different degrees of weathering (W1, W2, W4) and having terrestrial ages of 5500, 18700 and > 50'000 years, respectively. A slice of 10 mm was cut out of the meteorites. Out of theses slices rods were cut and the rods were divided into pieces. Pieces making up about 1 g were ground in a tungsten carbide ball mill and sieved to a size fraction finer 25 μm. The finest dust (<12 μm) was removed by sedimentation in acetone. Of the resulting size fractions 200 mg were contacted with 0.6 ml 40% nitric acid for 1 hour. The measurement of the released uranium by leaching the powder fractions were performed with a quadrupol ICP-MS.

Results: From each meteorite 3 positions were analyzed for U enrichments:

Surface exposed to air,
surface in contact to soil
an interior chip.

For the oldest investigated meteorite the sample in contact to the ground was highest in U contamination, for the two younger meteorites the surface sample exposed to the air were highest. The interior samples were lowest in U concentrations for all meteorites. In tab. 1 the values for the surface concentration in air minus the volume concentrations are given for the samples together with the measured carbon 14 ages and the calculated terrestrial ages taking the age of the meteorite JaH 078 as a basis.

Table 1 U enrichment on the surface of meteorite[1]

Sample	^{14}C age measured[2]	U surface enrichment	calculated terrestrial age
SaU 001	5500±1300	2.46ppb	6890 ± 2300
JaH 078	18700±1300	6.67ppb	18700
Dho 005	> 50'000	27.18ppb	76200 ±16100

Conclusions: Weathering of meteorites influencing their composition in hot deserts is controlled by temperature regime, humidity and local composition of the soil and the duration of all these processes. But the uptake of uranium is dominated by the duration of the transfer of U from soil to the meteorite surface leading to a proportionality of surface enrichment of U and terrestrial residence time. In contrast to carbon 14 ages the "U enrichment ages" are not limited to 50'000 years of exposure.

References: [1] Christian Stenger 2006, *Master Thesis* University of Bern pp 79 [2] Al-Kathiri et al. 2005. *Meteoritics & Planetary Science* 40:1215-1239

TERRESTRIAL ANALOGS FOR METEORITIC POROSITY MEASUREMENTS.

M. M. Strait[1], G. J. Consolmagno, S. J.[2] and D. T. Britt[3], [1]Alma College, Alma, MI 48801. E-mail: straitm@alma.edu. [2]Specola Vaticana, V-00120, Vatican City State. [3]University of Central Florida, Orlando, FL.

Introduction: Porosity is an important parameter in studying the evolution of bodies in the Solar System. We have been measuring the porosity of meteorites for a number of years using two methods: hand sample measurements using helium pycnometry [1] and thin section measurements using backscatter scanning electron microscopic images and a computer measurement program [2]. For most meteorite types measured there is good agreement between the two methods, however, the hand sample method must have the pore spaces empty of weathering products and accessible to the helium and the thin section method must have the porosity visible within the resolution of the imaging system [3]. Both methods can reliably measure porosities within the limitations of each method.

Ordinary chondrites and achondrites show agreement between the two methods within ±5% [4], however carbonaceous chondrites show significantly more porosity in the hand samples. This difference is still being explored and may be due to the complex texture of the fabric obscuring the porosity, or it could be in the nature of the minerals present in these meteorites.

Results: Herein we report another validation of our methodology. A suite of typical terrestrial rocks covering a wide range of rock classes and porosities has been measured using both methods. The rocks being measured include igneous rocks (porphyry, gneiss, gabbro, basalt, basalt breccia and anorthosite), metamorphic rocks (quartzite, schist, marble, chert breccia and slate) and sedimentary rocks (limestone, ferruginous sandstone, siliceous sandstone, shale and siltstone). Thin sections were from made from the same hand samples on which measurements were made. The porosities of the terrestrial rocks chosen match the range of porosities observed in the meteorites that have been measured. The metamorphic rocks show the lowest porosities ranging from 0.5% in quartzite to 2.3% in the schist. The igneous rocks were a fair amount of overlap with the metamorphic rocks, ranging from 0.7% in gneiss to 3.9% in anorthosite. Sedimentary rocks porosities are significantly higher, ranging from limestone at 3.7% to siltstone at 28%.

Appearances in the terrestrial samples tend to be similar to like porosities in meteorites. However, carbonaceous chondrites measured using hand samples show porosities ranging up to 25%, although the pore space is not as evident as that exhibited in terrestrial samples with porosities this high. In fact, thin section porosities and appearances of carbonaceous chondrites appear similar to the very low porosity samples such as quartzite.

Texture in terrestrial rocks is cleaner than that seen in meteorites and shows none of the weathering that fills in pore spaces in some meteorites. Published values for porosities in the suite measured here agree within the error ranges we have determined.

References: [1] Britt D. T. and Consolmagno G. J. 2003. *Meteoritics & Planetary Science* 38:1161-1180. [2] Strait M. M. et al. 1996. 27th Lunar & Planetary Science Conference. pp. 1285-1286. [3] Strait M. M. and Consolmagno G. J. 2004. *Meteoritics & Planetary Science* 39:A100. [4] Strait M. M. and Consolmagno G. J. 2005. Abstract #2073. 36th Lunar & Planetary Science Conference.

SUPERNOVA NIERITE (α-Si_3N_4) FROM MURCHISON.

R. M. Stroud[1], L. R. Nittler[2], and C. M. O'D. Alexander[2],. [1]Code 6360, Naval Research Laboratory, Washington, DC 20375, E-mail: stroud@nrl.navy.mil. [2]Dept. of Terrestrial Magnetism, Carnegie Institution of Washington, Washington, DC 20015.

Introduction: Meteoritic Si_3N_4 includes both solar and presolar grains. Silicon nitride grains found in enstatite condrites, e.g., Qingzhen (EH3) [1], Indarch (EH4) [2] are almost exclusively solar in origin, whereas those from ordinary and carbonaceous chondrites, e.g, Murchison (CM2), Tieschitz (H3.6) have isotopic signatures similar to SiC X grains, indicating an origin in Type II supernovae [3-6]. Two crystalline polytypes of meteoritic Si_3N_4 have been identified, nierite (α-Si_3N_4) and β-Si_3N_4, [7], however no structural data on supernova grains are yet published. We report here results from transmission electron microscopy (TEM) investigations of Si_3N_4 from Murchison, which indicate that the X-grain associated Si_3N_4 takes the nierite form.

Methods: We analyzed the CsF residue of Murchison of [4] using an EDAX particle analysis system on a JEOL 6500F SEM to identify SiC and Si_3N_4 grains on two mounts. We identified seven Si_3N_4 grains, ranging in size from 0.4 to 1.5 μm. Although isotopic data are not yet available, based on the previous studies on the same residue [4], we can be fairly certain that these are presolar supernova grains. Two of the new grains have an elongated, needle-like morphology, while the others appear blocky in the SEM. Sections for TEM studies were prepared using in-situ focused-ion-beam (FIB) lift-out with a FEI Nova 600 FIB. The TEM studies were performed with a JEOL 2200FS microscope, equipped with a Noran System Six energy dispersive spectroscopy (EDS) system and Gatan Ultrascan CCD.

Results: The Si_3N_4/SiC ratio of 10^{-3} is consistent with the results of [4] and with isotopic results on a new Murchison residue [8]. This is about 3 times higher than was previously found for residues prepared by HF/HCl [3, 6], suggesting that Si_3N_4 better survives the CsF treatment. Bright-field TEM imaging and diffraction studies of one of the sectioned grains reveal that it consists of two distinct, well-ordered crystals: one 150 nm x 100 nm and one 125 nm x 220 nm; both with the nierite structure (trigonal, a = 0.7758 nm, c = 0.5623 nm). The composition of the crystals measured by EDS is stoichiometric Si_3N_4.

Discussion: The formation of Si_3N_4 in Type II supernovae is poorly understood. The observed grain morphologies suggest formation under equilibrium condensation conditions, however calculations [9] indicate that Si_3N_4 is unstable with respect to SiC, TiN and AlN. Isotopic measurements to confirm the supernova origin of this grain and structural studies of additional Si_3N_4 grains are planned in order to better constrain the circumstellar condensation conditions.

References: [1] Lin, Y.T., S. Amari, and O. Pravdivtseva, 2002. *Astrophysical Journal* 575:257-263. [2] Russell, S.S., et al., 1995. *Meteoritics* 30:399-404. [3] Nittler, L.R., et al., 1995. *Astrophysical Journal* 453:L25-L28. [4] Nittler, L.R. and C.M.O'D. Alexander, 2003. *Geochimica Et Cosmochimica Acta*, 67:4961-4980. [5] Zinner, E., et al., 2003. Meteoritics & Planetary Science38:5106. [6] Hoppe, P., et al., 1996. *Geochimica Et Cosmochimica Acta* 60:883-907. [7] Lee, M.R., et al., 1995. *Meteoritics* 30:387-398. [8] Nittler, L.R., C.M.O.'D. Alexander, and A. Nguyen, 2006. *Meteoritics and Planetary Science*, this volume. [9] Lodders, K. and B. Fegley, 1995. *Meteoritics*, 30:661-678.

NUMERICAL MODELING OF TEKTITE ORIGIN IN VERTICAL IMPACTS.

V. V. Svetsov. Institute for Dynamics of Geospheres, Russian Academy of Sciences. E-mail: svetsov@idg.chph.ras.ru.

Introduction: Geochemical arguments show that tektites are derived from sedimentary layers at the earth surface [1–3]. Numerical simulations of ejecta motion after impacts [4] suggest that the Ries-moldavite strewn field could have been created by an oblique impact at angles 30–50º to the horizontal with a velocity of 20 km/s. In this case the melt of an upper 40 m thick layer is ejected downrange, moves through the atmosphere in a cloud of heated gas and lands at some distance from the crater as tektites. However, this is not the only way to explain the origin of tektites. It has been speculated that tektites can be produced in vertical impacts and move through a wake left by an impactor in the atmosphere [5]. Another possible mechanism (at least for layered Australasian tektites) is the melting of soils by radiant heating from aerial bursts [6]. In this study numerical simulations of ejecta motion were made for near-vertical impacts.

Numerical Approach: The modeling of impacts was based on hydrodynamic equations which were solved numerically by the SOVA method [7]. Tillotson equation of state was used for target materials and a tabulated equation of state for heated air. Tektites were treated as particles moving with melted materials after ejection from a growing crater and as small objects moving individually through the atmosphere at the later stage. The approach was in general similar to that used in [4]. It was assumed that the impact occurs at some small angle to the vertical but the flow was simulated approximately as axially symmetrical.

Results: The motion of a molten surface layer at relatively low impact velocities has some specific features. A sandy layer melts nearby the impact point and is ejected to the wake. The melt particles move at the top of a low-velocity (2-3 km/s) ejecta curtain along trajectories close to vertical. From altitudes above ~50 km they move ballistically through the wake filled by air heated to some thousands Kelvins and then through the upper atmosphere. This tektite-forming material spreads in the direction opposite to the impact direction (in contrast to oblique impacts) and lands in some area with a shape depending on the impact velocity and angle. Some selected impact parameters give the best fit to the size of the tektite strewn field and its distance from the Ries crater. The calculated mass of tektites is of the order of the mass obtained by geological estimates.

Conclusions: The simulations show that the moldavite strewn field could originate from impacts of asteroids about 1 km in size at angles 10–20º to the vertical with velocities from 11.2 km/s to about 13 km/s. Near-vertical impacts with higher velocities can produce more extensive tektite strewn fields.

Acknowledgments: This publication is based on work supported by Award No. RUG-2655-MO-05 of the U. S. Civilian Research and Development Foundation.

References: [1] Barnes V. E. 1990. *Meteoritics* 25:149–159. [2] Glass B. P. 1990. *Tectonophysics* 171:393–404. [3] Koeberl C. 2001. *GSA Special Paper* 293:133–151. [4] Stöffler D. et al. 2002. *Meteoritics & Planetary Science* 37:1893–1907. [5] Svetsov V. 2001. 6th ESF-Impact Workshop. pp. 127–128. [6] Wasson J. T. 2003. *Astrobiology* 3:163– 179. [7] Shuvalov V. 1999. *Shock Waves* 9:381–390.

Ar-Ar DATING OF SHOCK-MELTED H CHONDRITES.

T. D. Swindle, D. A. Kring, C. Isachsen, E. K. Olson, and J. R. Weirich, Lunar and Planetary Laboratory, University of Arizona, 1629 E. University Blvd., Tucson AZ 85721-0092 USA. E-mail: tswindle@u.arizona.edu.

As a part of our ongoing project to study shocked and shock-melted ordinary chondrites, we have used the ^{40}Ar-^{39}Ar technique to analyze 12 samples from three H chondrites. Our two main goals are to determine when major recent (<1 Ga) events happened and how the early impact history compares with that of the Moon, for which a cataclysmic bombardment ~4 Ga ago has been proposed.

For Gao-Guenie, a chondrite with impact melt veins, three of the six samples studied have four- or five-point low-temperature isochrons of 305 Ma to 360 Ma, and a fourth has a minimum apparent age of 310 Ma (the other two samples do not have any apparent ages that low). We interpret this as incomplete degassing in an impact event 310±25 Ma ago. At least three other H chondrites (of a total of 19 studied) contain evidence for an impact event between 270 Ma and 390 Ma [1, 2]. LaPaz Icefield 02240, an impact melt breccia, has clearly been partially degassed in an event <1100 Ma ago, but there are no apparent low-temperature isochrons or plateaus. Northwest Africa 2058, a meteorite that is >90% impact melt, also suffered an event in the last 500 Ma, but it is impossible to pin it down more precisely than that with the present data, even though we analyzed three samples.

As previously reported [3], all three samples of LAP 02240 have apparent plateau ages of ~4000 Ma (average of 3914±36 Ma), consistent with the lunar cataclysm, and roughly consistent with three other H chondrites. Gao-Guenie is the only other sample of those reported here that might contain information about early impacts. One sample appears to have a plateau at ~4300 Ma, which would make it a rare sample with a shock age between 4000 Ma and 4400 Ma. However, on closer inspection, the apparent ages in the “plateau” systematically rise, from ~4200 Ma to ~4400 Ma, suggesting a phase that was only partially degassed in the 300 Ma event [4].

References: [1] Bogard D. D. 1995. Meteoritics, 30, 244-268. [2] Folco L. et al. 2004. Geochimica et Cosmochimica Acta, 68: 2379-2397. [3] Swindle T. D. et al. 2006. 37th Lunar & Planetary Science Conference, Abstract #1454. [4] McDougall I. and Harrison T. M. 1999. Geochronology and thermochronology by the ^{40}Ar/^{39}Ar method. 2nd edition, New York: Oxford Univ., 269 pages.